Mon. Not. R. astr. Soc. (1988) **234,** 583–624

An optical spectrophotometric survey of abundances in Magellanic Cloud Planetary Nebulae

D. J. Monk, M. J. Barlow and R. E. S. Clegg *Department of Physics and Astronomy, University College London, Gower Street, London WC1E 6BT*

Accepted 1988 March 10. Received 1988 March 4; in original form 1987 December 21

Summary. Optical spectroscopic data for 71 Planetary Nebulae (PN) in the Large and Small Magellanic Clouds have been analysed. The line fluxes have been used to determine nebular temperatures, densities, and the abundances of He, N, O, Ne, and Ar, relative to H. In our sample there are 12 nebulae with $N/O \geq 0.5$, resembling Peimbert's Type I PN; six low-excitation (LE) objects [$1 \leq I(5007)/I(H\beta) \leq 4$]; and four very-low-excitation (VLE) nebulae [$I(H\beta) > I(5007)$], similar to the Galactic VLE class. Mean abundances have been calculated for the nebulae not in these special groups. After correction for collisional excitation contributions to the nebular He I lines, PN in the SMC and LMC yield mass fractions of $Y=0.249\pm0.025$ and $Y=0.258\pm0.015$, respectively. Compared with PN in our own Galaxy, the abundances of Ne and Ar, which are the elements in our sample least affected by nucleosynthesis, are lower by 0.6 and 0.35 dex for the SMC and LMC respectively. The oxygen and neon abundances in the Magellanic Cloud PN are the same as those previously found for H II regions in the LMC and SMC, but the nitrogen in PN is enhanced by 0.9 and 1.0 dex in each galaxy, respectively. This is found to be consistent with the processing of all of the original carbon to nitrogen by the CN cycle, operating in the progenitor stars at the time of the first dredge-up. This process seems to have operated much more efficiently in the metal-poor Magellanic Clouds than in the Milky Way, in agreement with theoretical predictions. Five Wolf–Rayet central stars are detected in the sample (two SMC, three LMC). The frequency of occurrence of these helium-rich central stars in low- and medium-excitation PN (15 per cent) is very similar to that of helium-rich white dwarfs in the solar neighbourhood, suggesting that events at the end of the AGB phase may be reponsible for the observed fractions of helium- and hydrogen-rich white dwarf stars.

1 Introduction

Early surveys of Magellanic Cloud planetary nebulae (Henize 1956; Lindsay 1961; Henize & Westerlund 1963; Lindsay & Mullen 1963; Westerlund & Smith 1964; Sanduleak, MacConnell &

Philip 1978; Jacoby 1980) and other early studies (Feast 1968; Webster 1969a, b, c; Smith & Weedman 1972) have provided identifications, colours, and kinematics for a large number of objects.

Spectroscopic studies of PN in the Large and Small Magellanic Clouds (LMC and SMC) followed this early work and provided an extension to the well-established and intensive investigations of PN within our own galaxy. Previous optical spectroscopic studies of Magellanic Cloud PN, though, have only been for relatively small samples (Osmer 1976; Webster 1976a, b, 1978; Dufour & Killen 1977; Aller *et al.* 1981; Aller 1983), as have the studies of Magellanic Cloud PN with IUE (Maran *et al.* 1982; Stecher *et al.* 1982; Barlow *et al.* 1983; Aller *et al.* 1987), and this has led to selection effects in the mean abundances derived for LMC and SMC PN.

In this paper, we report the results of an abundance analysis of the largest sample of optical spectrophotometric spectra so far obtained of Magellanic Cloud PN. Of the 74 nebulae observed, 71 are classifiable as PN. The 21 PN observed in the SMC represent about 70 per cent of those listed in the Sanduleak *et al.* (1978) catalogue, while the 50 PN observed in the LMC represent 50 per cent of those catalogued by Sanduleak *et al.* (1978). We will follow the standard practice for Galactic PN and adopt the earliest identification of any particular PN as the reference for its name. The catalogue of Sanduleak *et al.* (1978) contains a cross-index of these identifications.

2 Observations and calibration

2.1 OBSERVATIONS

The spectra discussed here were obtained from the AAO database, the original observations having been made by Dr E. J. Wampler with the 3.9-m Anglo–Australian Telescope (AAT) at Siding Spring Observatory during the nights of 1975 November 27/28 (low resolution data), and 1976 February 4/5, 5/6, 6/7 and 7/8 (medium resolution data), using the Boller and Chivens Spectrograph and Image Dissector Scanner (IDS) (Robinson & Wampler 1972), at the $f/15$ focus. The low resolution spectra were obtained with a 300 line mm^{-1} grating, giving a noise-limited useful wavelength range from 3600 to 7400 Å, at a resolution of ≈25 Å FWHM. The medium-resolution spectra were obtained with a 600 line mm^{-1} grating, giving a useful coverage of 3600–7100 Å, at a resolution of ≈12 Å FWHM. The low- and medium-resolution spectra were obtained with entrance slots of 1×2 and 1×1 mm^2, respectively, which gave projected areas on the sky of 3.6×7.2 $arcsec^2$ and 3.6×3.6 $arcsec^2$. Each object was observed for 2 min in each of two slots having a projected separation on the sky of 20 arcsec. The object spectra were then summed and the sky spectra, which had been recorded simultaneously in the alternative slots, were subtracted in order to yield net spectra. The sky spectra were monitored for the presence of field stars in the beam and when such cases occurred the relevant sky spectrum was replaced with that from the observation immediately before or afterwards. All of the low-resolution spectra were obtained on the night of 1975 November 27/28, when the PN were observed in essentially Right Ascension order. The same order of observation applied on the nights of the medium-resolution observations. The medium-resolution observations of the SMC PN N6, L239, L302, and L305 were obtained on February 7/8, while the remaining SMC medium-resolution data were obtained on February 5/6.

Using the SDRSYS reduction package at the AAO (Straede 1980), the spectra were calibrated in wavelength with respect to comparison exposures of a He–Ne arc, and were calibrated spectrophotometrically by observations of white dwarf stars from the list of Oke (1974). The subsequent analysis of the calibrated spectra was carried out at the UCL STARLINK node, using the DIPSO package of routines (Howarth & Murray 1987) to measure line intensities. Table 1(a–d) presents the measured line intensities on a scale where $I(H\beta)=100$, corrected for interstellar extinction and atmospheric dispersion as described below.

Table 1(a). Corrected relative line intensities for LMC PN: medium resolution.

λ(Å)	ID	N1 (LE)	N25 (VLE)	N42	N52	N60	N66	N77F	N78
3727	[OII]	< 29.0	58.9	< 101.0	< 31.0	< 32.0	< 86.0(60.6)a	279.4	28.6
3868	[NeIII]	< 28.0	< 19.0	< 119.0	67.0	45.7	103.1(112.2)a	87.3	38.2
3889	HeI,H8		33.3::		22.6	22.8			
3969	[NeIII],Hε	18.0		< 65.0	42.5	19.2	15.4	26.1	22.2
4101	Hδ	27.2	31.5	30.4	20.4	24.8	27.5	18.9	25.7
4340	Hγ	44.1	48.7	39.8	52.5	47.8	49.3	45.4	45.8
4363	[OIII]	8.9::	< 10.0	30.6	13.2	6.0	18.7	31.4	1.6::
4471	HeI				4.8	4.5			7.2
4542	HeII								
4686	HeII				23.8		60.2	68.1	
4712	HeI,[ArIV]				5.8		15.0		
4740	[ArIV]				5.3		8.7		
4861	Hβ	100.0	100.0	100.0	100.0	100.0	100.0	100.0	100.0
4959	[OIII]	128.6	17.4	448.3	418.0	222.4	319.0	453.5	186.5
5007	[OIII]	398.0	47.7	1403.8	1238.3	647.2	973.8	1382.8	549.1
5200	[NI]							10.5	
5411	HeII						5.8	9.5	
5755	[NII]		3.2				2.6	14.4	
5876	HeI	13.5	4.9	15.8	11.1	13.4	7.7	6.6	14.8
6300	[OI],[SIII]	1.5	2.5	11.9		2.8	10.0	30.6	2.5
6363	[OI]	0.9					3.5		
6548	[NII]	1.6	17.1	21.9	0.6	4.3	40.0	156.3	6.5
6563	Hα	282.3	282.8	282.6	282.7	282.4	282.2	283.4	281.2
6584	[NII]	4.6	49.8	63.8	1.6	12.7	117.0	460.9	18.9
6678	HeI	3.8		4.4	4.3	3.4			4.5
6717	[SII]						5.8	14.4	2.8
6731	[SII]			6.9		1.8	8.0		
	OIII RATIO:	59.1	6.7	60.6	125.2	145.7	69.0	58.4	456.1
	NII RATIO:		21.1				59.7	42.8	
	TEMP(OIII):	(10500)	(10500)	15750	11750	10900	15000	16200	(10500)
	TEMP (NII):						11000	13000	
	c′ :	0.45	0.88	0.64	−0.03	0.68	0.50	−0.27	0.80
									0.33

Table 1(a) – *continued.*

λ(Å)	ID	N99 (VLE)	N101 (VLE)	N102	N104A*	N110	N122	N123	N124	N125
3727	[OII]	769.3	53.5	55.8	< 206.0	72.7	52.6	37.5	34.8	38.5::
3868	[NeIII]	14.3::	29.2	99.3	100.6	83.9	125.8	38.5	67.0	40.3::
3889	HeI,H8					28.5	22.8	15.5	17.0	
3969	[NeIII],Hε			30.5	36.2::	50.0	50.0	24.5	36.7	22.8::
4101	Hδ	32.2	23.6	22.7	11.5	25.2	26.4	25.2	18.1	21.5
4340	Hγ	43.2	51.5	47.6	52.1	42.7	45.7	44.5	46.4	48.2
4363	[OIII]			45.7	25.1	9.8	19.0	6.1	21.8	11.3
4471	HeI			5.2		4.6	5.1	4.6	3.6	4.3
4542	HeII						2.4			
4686	HeII			75.3	39.1		42.0		23.1	
4712	HeI,[ArIV]			12.3			6.3	0.9	4.4	
4740	[ArIV]			17.5			9.3		3.0	
4861	Hβ	100.0	100.0	100.0	100.0	100.0	100.0	100.0	100.0	100.0
4959	[OIII]			380.0	525.0	429.9	367.9	229.1	521.6	341.9
5007	[OIII]	7.0	2.3	1124.8	1545.9	1198.3	1066.0	684.6	1512.6	1004.9
5200	[NI]			12.7			1.9			
5411	HeII			5.7			3.2		1.5	
5755	[NII]	3.2	2.9	9.0			8.3			
5876	HeI	2.0	1.2	11.8	9.9	15.2	15.3	13.3	10.6	14.8
6300	[OI],[SIII]		3.2	26.8	11.9	13.7	13.0	3.7	5.2	2.4
6363	[OI]				1.8	3.7	3.6		1.0	
6548	[NII]	46.8	29.7	117.5	28.7	14.1	85.2	7.8	7.0	4.8
6563	Hα	282.5	282.3	282.8	283.0	282.8	282.0	282.1	282.9	281.7
6584	[NII]	136.9	87.0	342.8	83.1	41.2	250.6	22.9	20.5	14.0
6678	HeI					5.4		3.2	3.6	5.2
6717	[SII]				6.1					
6731	[SII]			30.4	12.5	4.5	13.1	3.1	5.3	3.8
	OIII RATIO:			32.9	82.6	166.0	75.3	148.6	93.3	119.2
	NII RATIO:	56.9	40.4	51.4			40.7			
	TEMP(OIII):	(10500)	(10500)	23250	13750	10500	14400	11000	13000	12000
	TEMP (NII):			12000			13800			
	c′ :	0.50	0.40	0.67	1.18	0.26	0.02	0.29	0.30	1.10

Table 1(a) – *continued.*

λ(Å)	ID	N133	N141	N151	N153	N170	N178	N181	N182	N184
3727	[OII]	< 25.0(6.6)a	22.0	< 38.0	55.6	67.5	59.5	373.2	34.3	56.3
3868	[NeIII]	51.8::(37.8)a	41.6	73.0	99.1	94.2	84.6	92.8	50.5	110.5
3889	HeI,H8		10.6		29.5	34.0	20.7		11.8	
3969	[NeIII],Hε	53.2	28.1	47.3	35.1	33.2	42.1		35.3	32.5
4101	Hδ	26.2	18.9	22.9	31.1	20.2	26.8		24.0	15.5
4340	Hγ	47.6	37.4	43.2	43.1	41.3	38.8	36.1	44.7	38.8
4363	[OIII]	11.2	8.0	9.9	20.6	17.1	15.5	7.2	7.1	18.5
4471	HeI	4.4	4.4	4.9	4.0	4.2	2.9	5.8	4.0	3.7
4542	HeII									
4686	HeII				30.7	32.1	9.7	55.4		45.7
4712	HeI,[ArIV]				3.9	3.7	2.7		2.5	
4740	[ArIV]				4.5	5.9	2.9			
4861	Hβ	100.0	100.0	100.0	100.0	100.0	100.0	100.0	100.0	100.0
4959	[OIII]	251.1	344.7	331.2	478.9	499.4	463.8	160.8	262.8	487.7
5007	[OIII]	701.2	976.1	946.2	1444.6	1481.5	1394.8	472.4	799.0	1361.5
5200	[NI]							31.9		
5411	HeII				3.3	3.0	1.6	4.1		6.7
5755	[NII]							32.2		
5876	HeI	13.2	13.4	13.9	9.7	10.3	12.1	9.8	14.4	10.5
6300	[OI],[SIII]	4.3	2.6	4.3	9.2	16.4	7.0	75.6	3.7	9.7
6363	[OI]		0.8		2.3	4.1	2.3	23.3	0.9	
6548	[NII]	1.8	6.2	6.6	13.5	17.0	9.6	511.1	4.8	9.1
6563	Hα	282.9	282.6	281.3	283.3	282.1	281.1	281.8	282.3	281.5
6584	[NII]	5.1	18.1	19.2	39.4	49.7	28.3	1493.0	14.2	26.4
6678	HeI	2.8	3.6	4.8	2.8	4.8	2.4		3.4	4.2
6717	[SII]				1.3		1.1			3.5
6731	[SII]		3.2		4.3	11.4	3.9	113.2		3.9
	OIII RATIO:	85.1	164.9	128.6	93.2	115.8	119.6	87.5	148.8	100.1
	NII RATIO:							62.2		
	TEMP(OIII):	13250	10750	11500	13100	12100	11900	13500	11000	12750
	TEMP (NII):							10750		
	c′ :	0.26	0.54	0.49	0.54	0.68	0.12	0.58	−0.11 0.25	0.74

Table 1(a) – *continued.*

λ(Å)	ID	N199 (LE)	N201	N203	N207	N208	N209	N211	N212	N221 (WS42)
3727	[OII]	78.7	35.9	< 80.0(70.8)a	82.4	76.8	49.0	< 45.0	51.7	39.8
3868	[NeIII]	< 8.0	67.5	47.2	105.3	126.8	92.9	76.9::	37.0::	58.8
3889	HeI,H8		17.9			13.9	21.8			
3969	[NeIII],Hε	30.3	38.3		35.3	43.8	57.4	50.0	44.2	35.3
4101	Hδ	28.4	23.8	13.5	26.3	25.7	17.3	22.7	33.1	15.0
4340	Hγ	37.7	45.6	39.9	44.7	47.5	46.1	40.6	41.6	41.2
4363	[OIII]	3.6::	25.0	5.5	18.0	20.7	16.4	22.6	11.0	16.6
4471	HeI	4.3	2.9		5.2	4.0		4.4		3.6
4542	HeII						2.7			
4686	HeII		25.3		43.1	25.3	23.5			20.4
4712	HeI,[ArIV]		5.8		2.5	4.8	4.6	3.4		3.0
4740	[ArIV]		7.4			3.5	4.6	4.5		2.0
4861	Hβ	100.0	100.0	100.0	100.0	100.0	100.0	100.0	100.0	100.0
4959	[OIII]	52.5	407.2	278.6	473.7	549.7	481.4	460.0	248.6	513.7
5007	[OIII]	148.6	1144.7	800.0	1387.3	1556.6	1392.1	1337.5	768.0	1518.2
5200	[NI]		0.8			0.9				
5411	HeII		3.0		4.7	1.7	1.5			1.8
5755	[NII]	2.1::	0.8		1.5	1.1	0.6			2.0
5876	HeI	6.7	12.1	15.2	10.4	12.1	11.9	14.6	17.5::	11.4
6300	[OI],[SIII]	3.0	7.6	3.3	14.5	11.3	9.6	5.3		8.8
6363	[OI]		1.5		4.9	3.0	2.7			3.0
6548	[NII]	28.0	11.4	7.7	25.8	16.2	10.8	4.2	2.8	33.8
6563	Hα	281.5	281.4	282.4	281.4	282.8	281.9	283.3	281.0	281.8
6584	[NII]	82.0	33.5	22.3	75.2	47.4	31.4	12.2	8.3	99.0
6678	HeI	2.5	3.4		3.4	3.0	4.2	3.7		2.0
6717	[SII]	1.0	2.1			1.4	2.4	0.9		
6731	[SII]	1.7	5.5	5.3	15.3	6.3	5.3	3.1	2.6	8.9
	OIII RATIO:	55.2	62.0	194.9	103.3	101.9	114.2	79.6	92.7	122.0
	NII RATIO:	51.7	59.1		67.8	57.9	72.6			68.1
	TEMP(OIII):	(10500)	15500	10000	12500	12600	12000	14000	13250	11900
	TEMP (NII):		11000		10500	11250	10250			10500
	c′ :	0.29	0.43	1.07	0.80	0.42	0.66	0.89	0.03	0.16 0.64

Table 1(a) – *continued.*

λ(Å)	ID	LM1-27 (WS17)	LM1-61 (WS40)	LM1-62 (WS41)	S1 (LE)	N16 (VLE)	N47 (VLE)
3727	[OII]	107.4	< 29.0(21.8)a	42.1	201.5	749.1	620.6
3868	[NeIII]	85.7	57.6	120.6	< 39.0		
3889	HeI,H8		29.3				
3969	[NeIII],Hε	44.6	33.8	41.6			
4101	Hδ	16.9	16.0	24.9	27.5	21.3	
4340	Hγ	36.6	43.7	47.8	47.8	57.6	
4363	[OIII]	12.2	18.4	20.9	10.0::		
4471	HeI		2.2	4.0			
4542	HeII		2.1				
4686	HeII	12.3	66.0	15.0			
4712	HeI,[ArIV]		10.3	3.0			
4740	[ArIV]		6.1	3.0			
4861	Hβ	100.0	100.0	100.0	100.0	100.0	100.0
4959	[OIII]	415.5	343.2	529.2	91.5	8.7::	
5007	[OIII]	1224.8	993.8	1523.8	273.2	10.2::	
5200	[NI]						
5411	HeII		5.8	1.4			
5755	[NII]	2.3::					
5876	HeI	10.6	4.0	13.1	13.4		
6300	[OI],[SIII]	2.0	3.9	9.1			11.6::
6363	[OI]	1.5	3.0	1.7			
6548	[NII]	21.6	2.1	10.1	8.6	12.6	13.0
6563	Hα	282.1	281.3	282.6	282.5	282.0	281.0
6584	[NII]	63.0	6.3	29.5	25.2	37.0	38.0
6678	HeI			2.7			
6717	[SII]			5.5		22.0	
6731	[SII]	24.7				19.4	63.2
	OIII RATIO:	134.7	72.7	98.4	36.3		
	NII RATIO:	37.4					
	TEMP(OIII):	11500	14500	12750	(10500)	(10500)	(10500)
	TEMP (NII):						
	c′ :	0.92	0.05	0.47	0.06	0.33	0.50
			0.68	1.11			

Table 1(b). Corrected relative line intensities for LMC PN: low resolution.

λ(Å)	ID	N24	N28	N39	N42	N66	N97	N102	N104A	N107*
3727	[OII]	28.8	105.3	19.9	89.8	75.7	112.0	69.1	174.5	< 37.0
3868	[NeIII]	44.9	71.3	73.0	110.7	81.8	111.6	107.6	90.2	141.3
3969	NeIII,Hε	27.3	37.9	37.0	59.0	27.1	37.9	49.3	63.0	
4101	Hδ	24.0	35.9	27.2	26.5	28.8	19.8	30.6	23.1	13.6
4340	Hγ	44.2	42.5	41.5	36.7	53.2	43.4	41.4	46.5	30.5
4363	[OIII]	9.5	18.4	16.1	26.1	23.6	35.4	32.4	17.0	26.2
4471	HeI	5.1	2.8	1.8	3.4		3.4	4.9		
4640	NIII		6.6					5.4		
4686	HeII		46.8	18.1		66.0	59.5	67.1	38.6	37.6
4740	[ArIV]		7.7			17.5	8.1	15.4		
4861	Hβ	100.0	100.0	100.0	100.0	100.0	100.0	100.0	100.0	100.0
4959	[OIII]	271.6	398.4	351.2	403.0	296.9	351.5	352.8	444.4	519.3
5007	[OIII]	782.8	1131.2	1024.9	1162.7	842.8	1004.4	975.5	1223.6	1474.6
5200	[NI]						28.5	8.0		
5411	HeII		4.1			8.7	4.6	4.4	3.2	
5755	[NII]		3.8			3.2	11.4	11.2		
5876	HeI	12.2	9.0	12.0	11.6	5.4	11.4	11.0	8.8	14.6::
6300	[OI],[SIII]	1.1	12.6	3.2	9.7	6.0		23.7	12.3	9.0
6363	[OI]		5.1		4.0		18.7	9.2		2.8
6548	[NII]		60.4	2.5	11.4	43.0	175.5	119.9	22.7	10.1
6563	Hα	282.0	281.4	282.6	281.6	282.6	283.1	282.6	282.3	282.8
6584	[NII]		176.9	7.2	33.2	126.1	522.0	350.9	66.3	29.3
6678	HeI		2.1	2.5	3.8			3.5	3.1	
6725	[SII]		13.1	3.0	9.2	19.4	46.1	28.3	17.3	
7065	HeI	4.3	6.7	6.5	6.1	4.0	4.0	6.4	2.7	9.4
7135	[ArIII]	8.9	11.7	4.7	7.5	10.9	14.2	17.1	9.5	13.0
7325	[OII]		16.6	3.2	7.2	9.6	14.0	12.6	14.4	14.3
	OIII RATIO:	111.0	83.3	85.4	60.1	48.2	38.3	41.0	98.2	76.2
	NII RATIO:		61.6			52.5	61.1	41.9		
	TEMP(OIII):	12300	13750	13600	16000	17750	20500	19250	12750	14500
	TEMP (NII):		10750			11750	11000	13250		
	c′ :	0.29	0.31	0.35	0.47	0.13	0.34	0.43	0.57	1.45

Table 1(b) – *continued.*

λ(Å)	ID	N184	N186A	N188	N192	LM1-9 (WS 4)	LM1-27 (WS17)	WS12	WS16
3727	[OII]	71.2	97.4	156.9	80.7	48.6::	176.4	103.1	265.3
3868	[NeIII]	83.1	117.6	69.9	74.8	62.7	103.6	89.6	90.6
3969	NeIII,Hε	36.3	40.1	29.9	33.5	39.0	31.6	37.3	57.8
4101	Hδ	22.0	32.0	22.1	17.1	19.7	17.1	36.0	24.6
4340	Hγ	44.8	45.1	45.2	46.6	44.9	42.2	44.5	33.0
4363	[OIII]	18.7	11.5	17.4	18.1	18.2	23.3	13.0	12.3
4471	HeI	3.8	2.6					3.2	
4640	NIII					3.3			
4686	HeII	40.7	27.1	34.6	62.2	30.5	14.6	19.0	54.4
4740	[ArIV]	3.1		5.4	7.3	5.9	16.5		
4861	Hβ	100.0	100.0	100.0	100.0	100.0	100.0	100.0	100.0
4959	[OIII]	436.7	426.1	442.9	435.1	372.5	406.5	437.0	367.0
5007	[OIII]	1166.1	1197.0	1254.2	1119.5	1077.4	1169.0	1196.7	1039.2
5200	[NI]								
5411	HeII	1.3		1.5	4.5				
5755	[NII]								
5876	HeI	8.8	11.2	7.6	6.2	9.2	11.8	9.0	10.6
6300	[OI],[SIII]	7.9	10.6	12.2	9.4	4.4	10.8	6.8	19.5
6363	[OI]	2.2	3.6	4.3					12.4
6548	[NII]	5.0	10.7	20.9	5.0	3.9	23.4	10.6	36.8
6563	Hα	282.8	281.1	281.8	281.2	281.3	282.6	281.8	282.3
6584	[NII]	14.7	31.3	61.0	14.7	11.4	68.3	31.1	107.7
6678	HeI	2.3	1.6	2.2	2.5	3.3	3.7		
6725	[SII]	6.2	8.6	21.0	10.6	4.6	24.6	4.8	31.1
7065	HeI	3.1	3.8	3.6	3.4	2.5	2.7	4.1	
7135	[ArIII]	7.5	9.8	10.4	7.9	5.2	14.3	9.1	17.5
7325	[OII]	8.1	8.7	16.6	5.6	5.3		4.0	9.4
	OIII RATIO:	85.6	141.3	97.8	86.0	79.7	67.5	125.7	114.7
	NII RATIO:								
	TEMP(OIII):	13500	11300	12900	13600	14000	15000	11800	12150
	TEMP (NII):								
	c′ :	0.49	0.58	0.50	0.47	0.53	0.55	0.41	0.40

Table 1(c). Corrected relative line intensities for SMC PN: medium resolution.

λ(Å)	ID	N1 (LE)	N4	N6	N70	N87	L66*
3727	[OII]	36.0	< 62.0(13.9)a	< 32.0(12.5)a	27.6::(85.6)a	< 38.0(16.9)a	< 101.0(84.9)a
3868	[NeIII]	< 16.0	26.2::(37.8)a	< 91.0(68.8)a	13.8::(26.1)a	41.1(31.2)a	< 102.0(53.7)a
3889	HeI,H8					15.6	
3969	[NeIII],Hε	31.1	41.7	< 47.0	24.5	20.9	49.0
4101	Hδ	29.7	30.4	18.9::	24.2	25.6	36.6
4340	Hγ	45.0	44.7	47.8	50.8	47.4	56.6
4363	[OIII]	2.7::	9.9(9.5)a	14.8	6.0	8.7	10.3(14.6)a
4471	HeI	5.7		6.6	8.2	3.1	(2.5)a
4542	HeII						
4686	HeII		8.7				70.9
4712	HeI,[ArIV]					2.7	
4740	[ArIV]						
4861	Hβ	100.0	100.0	100.0	100.0	100.0	100.0
4959	[OIII]	64.8	277.1	270.6	154.9	203.3	348.8
5007	[OIII]	200.0	924.7	762.8	457.0	617.1	1062.4
5200	[NI]						
5411	HeII						
5755	[NII]						
5876	HeI	8.8	18.6	15.5	12.4	15.6	
6300	[OI],[SIII]				1.6	2.0	
6363	[OI]						
6548	[NII]	5.5	1.2	7.9	5.0	1.4	11.0
6563	Hα	282.0	282.6	280.7	281.5	281.5	281.7
6584	[NII]	16.1	3.7	23.0	14.7	4.2	32.5
6678	HeI	3.7		4.9	2.6	3.9	
6717	[SII]				1.8		
6731	[SII]						
	OIII RATIO:	97.7	121.4	69.9	101.7	94.8	136.8
	NII RATIO:						
	TEMP(OIII):	(10500)	12000	14500	10900	13000	11750
	TEMP (NII):						
	c′ :	0.20	−0.07	0.77	0.23	0.09	−0.14

Table 1(c) – *continued.*

λ(Å)	ID	L239	L302 (VLE)	L305*	L536	N8 (VLE)
3727	[OII]	71.3::(32.4)a	272.7	< 518.0(29.9)a	66.3::(29.0)a	484.3
3868	[NeIII]	62.2(70.2)a		< 310.0(82.6)a	< 112.0(66.7)a	
3889	HeI,H8					
3969	[NeIII],Hε	39.2		123.4		
4101	Hδ	27.8	22.7	15.2	11.9	63.2
4340	Hγ	47.8	51.1	50.5	46.3	52.8
4363	[OIII]	17.9(12.6)a		(20.7)a	12.8	
4471	HeI	3.7				
4542	HeII					
4686	HeII	49.8		40.9	52.1	
4712	HeI,[ArIV]				12.8	
4740	[ArIV]				6.5	
4861	Hβ	100.0	100.0	100.0	100.0	100.0
4959	[OIII]	321.7	23.2	204.3	82.8	
5007	[OIII]	955.0	63.8	642.7	287.7	
5200	[NI]				3.7	
5411	HeII					
5755	[NII]				7.2	
5876	HeI	10.3		11.6	18.6	
6300	[OI],[SIII]	5.1				
6363	[OI]					
6548	[NII]	4.0	35.3	40.2	52.8	14.7
6563	Hα	281.6	283.2	281.4	282.5	281.9
6584	[NII]	7.3	103.5	117.2	154.9	42.9
6678	HeI	3.2		14.0	5.4	
6717	[SII]				11.1	32.1
6731	[SII]					
	OIII RATIO:	71.2		40.9	28.8	
	NII RATIO:				29.0	
	TEMP(OIII):	12700	(10500)	19600	24600	(10500)
	TEMP (NII):				17200	
	c′ :	−0.02	0.33	0.79	0.16	0.63
		0.65				

Table 1(d). Corrected relative line intensities for SMC PN: low resolution.

λ(Å)	ID	N1 (LE)	N2	N5	N6	N7	N18	N29 (LE)
3727	[OII]	33.8	7.9	66.0	< 22.0(12.5)a	10.7	12.1::	210.9
3868	[NeIII]	< 7.0	48.8	71.3	38.2(68.8)a	25.6	34.4	< 54.0
3969	NeIII,Hε	10.2	18.7	28.6	24.5	17.2	27.5	
4101	Hδ	23.2	18.0	22.3	20.7	13.6	29.9	19.6
4340	Hγ	48.4	38.0	43.9	46.7	43.1	52.4	52.1
4363	[OIII]	3.9::	12.8	18.6	17.7	8.1	6.9	
4471	HeI	3.1	2.0	4.2	4.4	4.1		
4640	NIII	1.0			1.6			
4686	HeII		25.4	40.0				
4740	[ArIV]							
4861	Hβ	100.0	100.0	100.0	100.0	100.0	100.0	100.0
4959	[OIII]	65.2	314.2	377.9	285.8	217.3	270.6	108.2
5007	[OIII]	188.8	862.7	1031.4	801.3	629.6	766.7	310.9
5200	[NI]							
5411	HeII		2.0	2.1				
5755	[NII]				1.9			1.0
5876	HeI	9.5	9.8	8.6	12.9	12.8	10.6	10.1
6300	[OI],[SIII]	2.1	2.8	5.8	3.7			5.1
6363	[OI]	1.1	1.8	1.9	1.2			1.1
6548	[NII]	5.4		8.2	9.0			
6563	Hα	281.7	281.1	282.7	282.5	281.7	282.2	281.8
6584	[NII]	15.8		23.9	26.2			
6678	HeI	3.2		3.4	5.0	4.6		
6725	[SII]		2.9	8.0	2.0		5.3	7.9
7065	HeI	4.3	5.8	4.7	10.5	6.2	3.7	6.0
7135	[ArIII]	4.2	4.2	5.5	6.8	2.3	6.0	9.0
7325	[OII]	21.6	2.2	7.7	8.1	3.4		12.8
	OIII RATIO:	65.0	92.1	75.9	61.3	104.7	149.6	
	NII RATIO:				18.2			
	TEMP(OIII):	(10500)	13250	14250	15250	12500	11000	(10500)
	TEMP (NII):							
	c′ :	0.38	0.40	0.34	0.74	0.49	0.33	0.95

Table 1(d) – *continued.*

λ(Å)	ID	N38	N40	N42 (LE)	N43	N44	N47 (LE)
3727	[OII]	36.2	57.8	145.1	12.5::(12.5)a	22.4	85.7
3868	[NeIII]	65.9	83.3	< 35.0	48.6	81.8	24.6
3969	NeIII,Hε	34.6	30.7		24.0	34.2	25.3
4101	Hδ	26.7	27.9	27.3	29.1	24.9	27.6
4340	Hγ	46.4	44.6	54.4	50.2	45.2	49.5
4363	[OIII]	11.5	10.8	5.5::	9.4	10.8	2.4::
4471	HeI	3.6			5.8	6.0	4.6
4640	NIII		2.7				
4686	HeII		34.8				
4740	[ArIV]						
4861	Hβ	100.0	100.0	100.0	100.0	100.0	100.0
4959	[OIII]	294.5	325.8	61.8	211.1	313.5	106.8
5007	[OIII]	825.9	911.5	158.2	617.6	881.4	293.7
5200	[NI]						
5411	HeII						
5755	[NII]						
5876	HeI	11.9	8.1	10.5	14.3	12.5	12.6
6300	[OI],[SIII]	3.0	2.5		2.5	2.3	3.4
6363	[OI]				1.2	1.1	
6548	[NII]			4.9			4.8
6563	Hα	282.8	282.0	281.1	281.3	282.6	283.0
6584	[NII]			14.5			14.0
6678	HeI	3.4			2.3	2.2	2.8
6725	[SII]				0.8		
7065	HeI	8.5		5.3	10.0	6.2	8.7
7135	[ArIII]	3.7	4.6		4.0	4.0	6.8
7325	[OII]	4.2		13.4	6.1		18.4
	OIII RATIO:	97.0	114.8	39.7	88.2	110.4	170.3
	NII RATIO:						
	TEMP(OIII):	12750	12250	(10500)	13250	12250	(10500)
	TEMP (NII):						
	c′ :	0.32	0.16	0.51	0.63	0.32	0.51

2.2 BLENDS

Several groups of lines were only partially resolved in both series of spectra, most importantly the [N II] 6548 Å, 6584 Å and Hα lines, and the Hγ and [O III] 4363 Å lines, which are used either for the determination of the effects of interstellar extinction and atmospheric dispersion, or as temperature diagnostics. To deconvolve these lines into their respective components we used the DIPSO routine ELF written by Dr P. J. Storey. The Gaussian emission line fits were constrained by the wavelength differences of the theoretical line centres, and by the requirement that all components should have identical FWHMs. The actual value of the FWHM was not constrained within the routine but fits were only accepted for FWHMs within $\approx$3 Å of the FWHM of the unblended lines in the spectrum.

The fitting was made more complicated by the presence of broad wings on the stronger lines (relative intensity $\geq$Hβ for a typical PN), which are a feature of the detector itself, and whose width increased with increasing line intensity. It was necessary, therefore, to estimate the FWHM of this broad component from the (unblended) Hβ line, and fit both a narrow and broad component to the strong lines within the blends. Examples of the fits for the [N II], Hα blend and for the Hγ, [O III] blend, for both the low- and the medium-resolution spectra, are given in Figs 1 and 2.

In the medium resolution spectra, the [N II], Hα blend and the Hγ [O III] blend are almost resolved by the instrument, and the estimated errors for the line fitting are in the range 5–15 per cent, depending on the relative strength of the components involved. There was more significant blending, however, in the low resolution spectra, and errors of about 10–30 per cent are estimated. It should be noted that the Hγ, [O III] blending was particularly pronounced in the low resolution spectra, and the weakest [O III] 4363 Å relative line intensities have the largest associated errors. Relative intensities for [O III] 4363 Å of less than 5 (on a scale where Hβ=100) have been designated as 'very uncertain' (::) in Table 1(a–d), and have not been used to calculate an electron temperature.

2.3 ATMOSPHERIC DISPERSION AND INTERSTELLAR EXTINCTION CORRECTIONS

Since the seeing was generally of the order of the entrance slit width, and because some nebulae were observed at large zenith distances, the spectra were affected by wavelength-dependent atmospheric dispersion. The effect of this is similar to that of interstellar extinction, and it was found necessary to correct for the two effects together. The spectra were first corrected to the Case B theoretical Hα:Hβ intensity ratio of 2.85 for T_e=10^4 K and n_e=10^4 cm^{-3} (Brocklehurst 1971; Hummer & Storey 1987), using a galactic reddening law curve (Howarth 1983) with a suitable value for the logarithmic extinction at Hβ [c' in Table 1(a–d)]. This correction is based on the assumption that both effects have the same wavelength variation between Hα and Hβ, and we are thus unable to make an estimate of the true interstellar extinction suffered by each object. Where objects were observed twice at the same resolution both values of c' are given.

The effects of atmospheric dispersion were most pronounced at the blue end of our spectra and further corrections were found to be necessary to the fluxes of the lines shortwards of 4400 Å. In order to estimate the magnitude of the corrections needed, we made two types of comparison. First, the relative intensities, following dereddening by c', of [O II] 3727 Å and [Ne III] 3868 Å, were compared with the dereddened relative intensities for these lines from Aller *et al.* (1981), Aller (1983) and Barlow (1987) for the nebulae in common. The relevant line fluxes are listed in Table 3(a) (LMC PN), and (b) (SMC PN). A summary of the mean ratios of the IDS intensities to the other intensities is presented in Table 4. Secondly, the Hγ:Hβ, and Hδ:Hβ ratios obtained from the IDS spectra, after dereddening by c', were compared with the theoretical ratios for

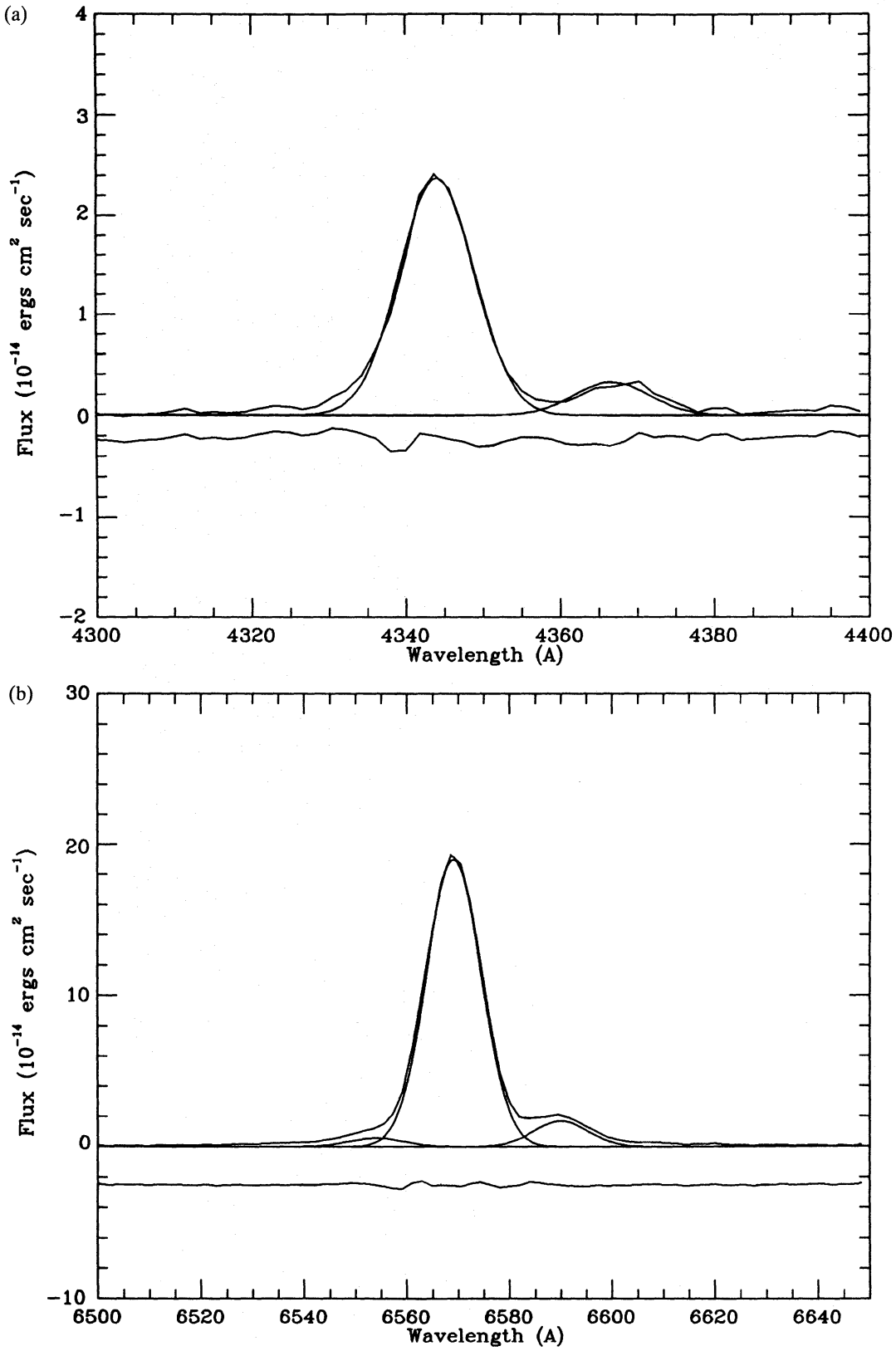

Figure 1. Examples of multicomponent fits to the Hγ, [O III] 4363 Å blend [top diagram (a)], and the Hα, [N II] 6548, 6584 Å blend [bottom diagram (b)] for a typical medium resolution spectrum. The spectral data and the Gaussian fits to each line are shown along with the residual (which is displaced downwards from zero for clarity).

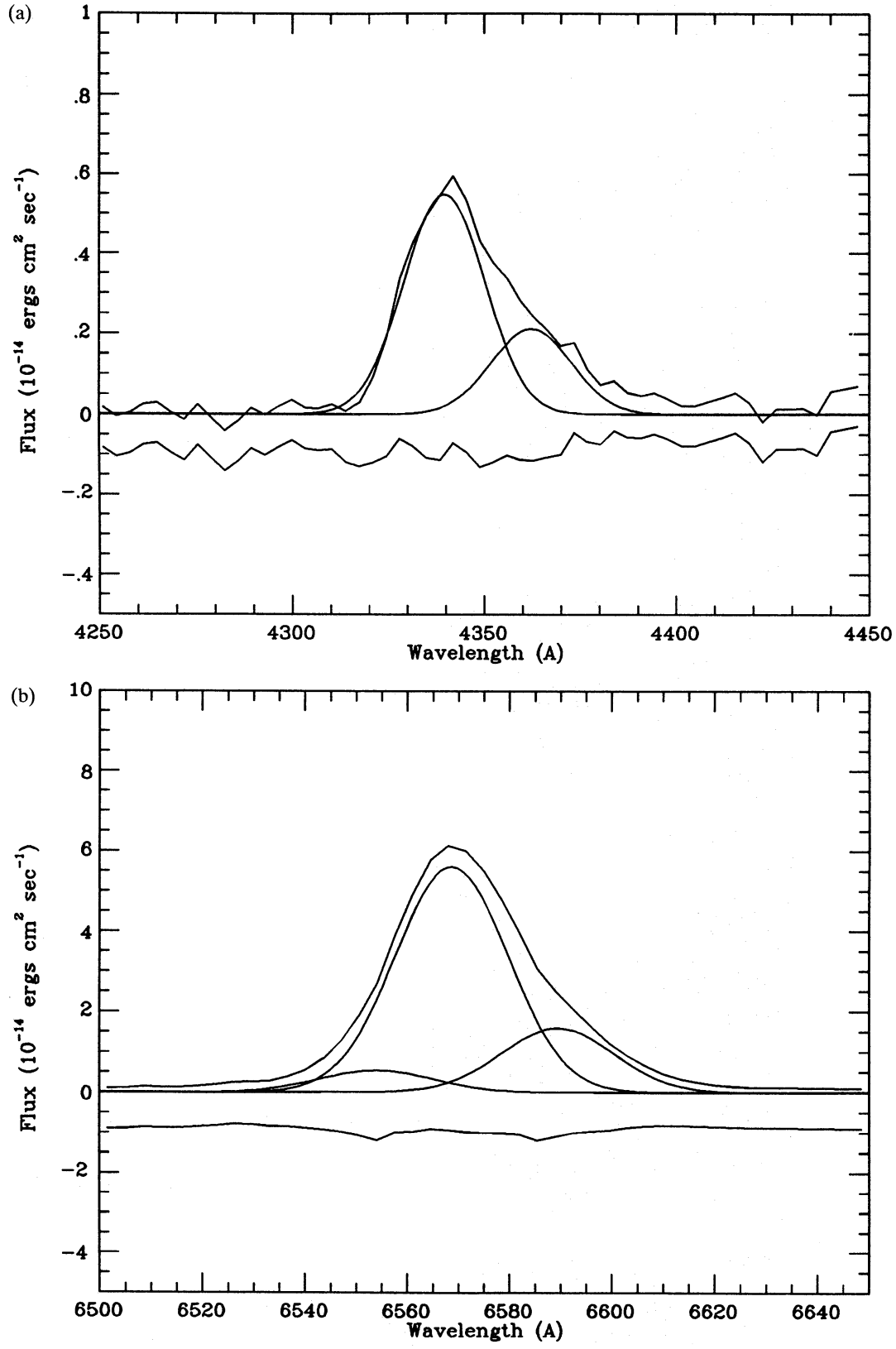

Figure 2. Examples of multicomponent fits to the Hγ, [O III] 4363 Å blend [top diagram (a)], and the Hα, [N II] 6548, 6584 Å blend [bottom diagram (b)] for a typical low resolution spectrum. The spectral data and the Gaussian fits to each line are shown along with the residual (which is displaced downwards from zero for clarity).

$T_e=10^4$ and $n_e=10^4$ cm^{-3}, which are equal to 0.469 and 0.259, respectively (Brocklehurst 1971). A comparison between the observed mean ratios and theoretical ratios is also included in Table 4.

Inspection of the various ratios in Table 4, for the low-resolution spectra of both the SMC and LMC PN, indicates that the corrections needed for the [O II], [Ne III], Hδ, Hγ fluxes are similar. The weighted mean of all 93 low resolution ratios (IDS divided by other) is 0.89. We have therefore multiplied all low resolution line fluxes between 3700 and 4400 Å by a factor of 1/0.89 (=1.12). The corrected low resolution line fluxes listed in Table 1(b) and (d) are thus the result of the dereddening of all fluxes by c', followed by multiplication by a factor of 1.12 for those lines with $\lambda<4400$ Å.

In the case of the medium-resolution spectra, comparison of the dereddened and intrinsic Balmer line ratios in Table 4 indicates that a correction factor of 1/0.89 (=1.12) is again appropriate for Hδ and Hγ, for both the SMC and LMC PN. However, in the case of the [O II] and [Ne III] lines, the ratio of the medium resolution IDS intensities to others is significantly lower than 0.89. We attribute this to the fact that these lines fall closer to the detector edge in the medium resolution spectra, and the sensitivity of the detector in its outer regions is significantly lower than in the central regions, due to pincushion distortion in the electrostatically focused image tube chain. On the basis of Table 4, we adopt a medium resolution spectra correction factor of 1/0.70 (=1.43) for lines with $3700<\lambda<4000$, and a correction factor of 1/0.89 (=1.12) for lines with $4000<\lambda<4400$ Å. The corrected medium resolution line fluxes listed in Table 1(a) and (c) are thus the result of the dereddening of all fluxes by c', followed by multiplication of the above correction factors.

The final corrected relative line intensities (on a scale where Hβ=100) are presented separately for the medium and low resolution spectra of the LMC PN [Table 1(a) and (b), respectively], and the SMC PN [Table 1(c) and (d), respectively]. The estimated errors of measurement of the relative line intensities are listed in Table 2, and are a function of (a) the wavelength, (b) the line intensity (relative to Hβ), and (c) the overall strength of the signal. These effects will combine to produce a specific signal-to-noise ratio for an individual line within a spectrum, and the estimated errors are the uncertainties due to the noise over the various wavelength regions. Spectra with a weak overall signal have higher associated uncertainties and these spectra have been labelled by an asterisk next to the object name in Table 1(a–d). For these spectra, and for other spectra with non-detections of the important [O II] 3727 Å and [Ne III] 3868 Å lines, upper limits to the fluxes in these lines were measured. For some nebulae for which only upper limits for [O II] 3727 Å or [Ne III] 3868 Å could be derived, the relative intensities of the lines were available from the higher resolution IPCS data of Barlow (1987). In such cases, the relative intensities from the latter source are given in parentheses (labelled with an 'a') following the upper limits derived from the IDS spectra [Table 1(a–d)], and were used subsequently for the derivation of the O^+ and/or Ne^{2+} abundances.

Rosa (1985) has found evidence that the IDS detector at ESO is non-linear, such that the detected signal, S, depends upon the input flux, I, as $S\propto I^{\alpha}$, with $\alpha\sim1.04$. We have used our

Table 2. Estimated errors in line intensity measurements due to the uncertainty in the continuum level caused by noise.

Relative Intensity	Wavelength Range (Angstroms)			
(Hβ = 100)	< 3900	3900-4200	4200-6000	6000-7000
3-5	> 50%	> 50%	40%	30%
5-15	"	30-40%	20-30%	20%
15-35	"	25%	10-15%	15%
>35	> 30%	10%	10%	10%

Table 3(a). Medium- and low-resolution spectra of LMC PN, corrected by c' only, compared to dereddened relative line intensities from Aller (1983; or Maran *et al.* 1982), and Barlow (1987).

		Relative Intensity (Hβ = 100)			
LMC	Line	Medium	Low	Aller (1983)	Barlow (1987)
N24	[OII]3727 Å	-	25.7	25.1	-
	[NeIII]3868 Å	-	40.1	42.9	-
N28	[OII]3727 Å	-	94.0	-	65.8
	[NeIII]3868 Å	-	63.7	-	87.3
N42	[OII]3727 Å	<70.6	80.2	-	-
	[NeIII]3868 Å	<83.3	98.8	-	-
N66	[OII]3727 Å	<60.3	67.6	-	58.7
	[NeIII]3868 Å	72.1	73.0	-	113.0
N97	[OII]3727 Å	-	100.0	116.4	118.6
	[NeIII]3868 Å	-	99.6	92.6	128.9
N102	[OII]3727 Å	39.0	61.7	72.0	63.4
	[NeIII]3868 Å	69.5	96.1	85.5	135.4
N104	[OII]3727 Å	<144.2	155.8	-	-
	[NeIII]3868 Å	70.4	80.6	-	-
N110	[OII]3727 Å	50.8	-	-	56.0
	[NeIII]3868 Å	58.7	-	-	106.8
N133	[OII]3727 Å	26.2	-	-	7.0
	[NeIII]3868 Å	32.2	-	-	39.5
N141	[OII]3727 Å	15.4	-	-	35.3
	[NeIII]3868 Å	29.1	-	-	69.5
N153	[OII]3727 Å	38.9	-	65.0	57.7
	[NeIII]3868 Å	69.3	-	97.7	100.5
N178	[OII]3727 Å	41.6	-	49.4	52.0
	[NeIII]3868 Å	59.2	-	82.9	102.2
N184	[OII]3727 Å	39.3	63.5	71.3	84.9
	[NeIII]3868 Å	77.3	74.2	64.5	98.6
N201	[OII]3727 Å	25.1	-	-	39.0
	[NeIII]3868 Å	47.2	-	-	92.3
N203	[OII]3727 Å	55.9::	-	-	74.9
	[NeIII]3868 Å	33.0	-	-	42.0
LM1-27	[OII]3727 Å	75.1	157.5	-	-
	[NeIII]3868 Å	60.0	92.5	-	-
LM1-61	[OII]3727 Å	<20.6	-	22.0: (Maran)	22.8
	[NeIII]3868 Å	40.2	-	47.9 (Maran)	63.2

observed [O III] 5007:4959 ratios (Table 1) to investigate whether such an effect is present also in the AAT IDS. The theoretical intensity ratio of these two lines is 2.88 (Nussbaumer & Storey 1981), while the mean 5007:4959 ratio given by the 68 medium- and low-resolution spectra with I(5007)/I(Hβ)>4 is found to be 2.90±0.12, implying that α=1.007±0.040. We conclude that our data do not provide evidence for significant non-linearity in the AAT IDS.

3 Nebulae with Wolf–Rayet central stars

The spectra of five of the planetary nebulae in our sample were found to show strong Wolf–Rayet emission lines, notably the C IV 5806 Å feature and the broad complex between 4650 and 4686 Å due to C III, C IV and He II. The Wolf–Rayet central star of LMC N203 was originally discovered by Feast (1968), while the presence of Wolf–Rayet central stars in SMC N6, SMC L302, LMC N110 and LMC N133 was first noted by Dr E. J. Wampler (1978, private communication).

The most recent systematization of the classification criteria for WC Wolf–Rayet stars is that by Torres, Conti & Massey (1986). Their assignments to a given subclass are based on the ratios of

Table 3(b). Medium- and low-resolution spectra of SMC PN, corrected by c' only, compared to dereddened relative line intensities from Aller *et al.* (1981) and Barlow (1987).

SMC	Line	Relative Intensity (Hβ = 100) Medium	Low	Aller *et al.* (1981)	Barlow (1987)
N2	[OII]3727 Å	-	7.1	24.5	29.0
	[NeIII]3868 Å	-	43.6	49.9	73.1
N4	[OII]3727 Å	<43.4	-	-	14.2
	[NeIII]3868 Å	18.3	-	-	38.5
N5	[OII]3727 Å	-	59.0	80.0	72.7
	[NeIII]3868 Å	-	63.7	87.0	78.4
N6	[OII]3727 Å	<22.1	<19.3	-	13.9
	[NeIII]3868 Å	<63.3	34.1	-	74.2
N8	[OII]3727 Å	338.7	-	-	528.0
	[NeIII]3868 Å	nd	-	-	2.4
N38	[OII]3727 Å	-	32.3	-	19.2
	[NeIII]3868 Å	-	58.8	-	51.7
N40	[OII]3727 Å	-	51.6	-	29.8
	[NeIII]3868 Å	-	74.4	-	68.6
N43	[OII]3727 Å	-	11.2::	14.4	12.9
	[NeIII]3868 Å	-	43.4	34.8	40.4
N44	[OII]3727 Å	-	20.0	25.5	21.4
	[NeIII]3868 Å	-	73.0	76.0	67.8
N70	[OII]3727 Å	19.3::	-	62.0	85.6
	[NeIII]3868 Å	9.6::	-	19.4	26.1
N87	[OII]3727 Å	<26.8	-	18.8	17.5
	[NeIII]3868 Å	28.8	-	27.5	33.6
L66	[OII]3727 Å	<70.6	-	-	101.4
	[NeIII]3868 Å	<71.1	-	-	64.1
L302	[OII]3727 Å	190.7	-	-	462.0
	[NeIII]3868 Å	nd	-	-	nd

the equivalent widths of (a) C IV 5806 Å to C III 5696 Å, and (b) C III 5696 Å to O V 5590 Å. Their sample consisted of bright Population I WC stars, whereas the five WC central stars in our sample are all extremely faint, with the consequence that O V 5590 Å was not detectable in any of the spectra, and C III 5696 Å was definitely detected only in the spectrum of SMC L302. Therefore, we have used only the ratio of the intensity of C IV 5806 Å to C III 5696 Å to classify the central stars. Table 5(a) lists, for each WC subclass, the mean value of this ratio, and its 1σ limits, as defined by Torres *et al.* (1986). Table 5(b) lists the observed ratio (or lower limit) of C IV 5806 Å to C III 5696 Å for each of the five WC central stars. The central stars of SMC L302 and LMC N110 are found to have spectral types of WC8 and WC4, respectively, while the remaining three central stars have spectral types WC4/5.

Mendez *et al.* (1986) have found that the spectral types of WC central stars in Galactic PN show a pronounced gap, in that the subtypes WC5, WC6 and WC7 do not occur. The spectral types found here are consistent with the same situation holding for central stars in Magellanic Cloud PN, although the presence of WC5 spectral types amongst them cannot be excluded as yet.

The spectra of WC central stars in planetary nebulae are known to be very similar to those of the much more luminous Population I WC stars which have the same spectral types (e.g. Smith & Aller 1971; Mendez *et al.* 1986). Since the spectra of WC stars contain no lines due to hydrogen, one must conclude that hydrogen-shell burning is excluded as the energy source for WC central stars, leaving helium-shell burning as the likely energy source. Wood & Faulkner (1986) have calculated helium-shell burning evolutionary tracks for PN central stars (however, their models

Table 4. Comparison of IDS relative intensities (corrected by c' only) with other sources.

Compared Data Sets (see notes below)	Sample Size	Compared Lines	Mean Ratio
B87/AL81	10	[OII]3727,[NeIII]3868	109.4±23%
B87/AL83	12	[OII]3727,[NeIII]3868	117.9±24%
SMC Low/Theory	11	Hγ/Hβ	90.0±8.5%
SMC Low/Theory	11	Hδ/Hβ	82.6±17%
LMC Low/(AL83 or B87)	12	[OII]3727,[NeIII]3868	93.6±20%
LMC Low/Theory	17	Hγ/Hβ	81.2±10%
LMC Low/Theory	17	Hδ/Hβ	85.3±22%
SMC Med/Theory	10	Hγ/Hβ	90.8±6.8%
SMC Med/Theory	10	Hδ/Hβ	93.4±50%
LMC Med/(AL83 or B87)	19	[OII]3727,[NeIII]3868	68.3±15%
LMC Med/Theory	39	Hγ/Hβ	84.4±8.3%
LMC Med/Theory	38	Hδ/Hβ	80.7±19%

Notes to Table 4.
B87 : Barlow, 1987
AL81 : Aller *et al.* , 1981
AL83 : Aller, 1983
Low : Low resolution data this paper
Med : Medium resolution data this paper
Theory : Brocklehurst, 1971

still had inert hydrogen shells above the helium layers). They found that helium-shell burning models evolved much more rapidly than hydrogen-shell burning models of the same mass. For example, after 3000 yr, a 0.6 $M_\odot$ hydrogen-shell burning model reached an effective temperature of 30 000 K at constant luminosity, whereas in the same time a 0.6 $M_\odot$ helium-shell burning model reached an effective temperature of 70 000 K, and experienced a luminosity decline of a factor of 2 compared with its starting value.

If nebular expansion velocities are independent of whether central stars are hydrogen- or helium-shell burning, then a consequence of the faster evolution in the latter case should be that at the same effective temperature the nebulae surrounding WR central stars should be younger and denser. The [O II] nebular electron densities measured by Barlow (1987) for the five PN with WC central stars are listed in the last column of Table 5(b). It is notable that all four of the early-WC central stars have nebular electron densities in excess of $10^4\,cm^{-3}$. Of the other 27 Magellanic Cloud PN in the survey of Barlow (1987), only one (SMC N54) was found to have an electron density larger than $10^4\,cm^{-3}$.

The only PN in our sample having a late WC central star, SMC L302, has a much lower nebular electron density ($930\,cm^{-3}$) than do the four early-WC central stars. Amongst Galactic PN, NGC 40 is the only nebula with a WC8 central star (Mendez *et al.* 1986) and its [O II] nebular electron density is also relatively low ($1400\,cm^{-3}$; Clegg *et al.* 1983). This may indicate that WC8 central stars have a somewhat different evolutionary origin from the early-WC central stars.

Table 5(a). Wolf–Rayet WC spectral classification (from Torres *et al.* 1986).

Class	log (C IV 5806 Å :C III 5696 Å)
WC 8	-0.26 ± 0.15
WC 7	$+0.22 \pm 0.16$
WC 6	$+0.74 \pm 0.29$
WC 5	$+1.08 \pm 0.20$
WC 4	$+1.84 \pm 0.22$

Table 5(b). Observed line strength ratio of C IV 5806 Å: C III 5696 Å.

Object	log (C IV 5806 Å :C III 5696 Å)	Class	n_e(O II)
SMC N6	> 1.23	WC 4/5	26600
SMC L302	−0.10	WC 8	930
LMC N110	> 1.61	WC 4	13000
LMC N133	> 1.34	WC 4/5	66000
LMC N203	> 1.57	WC 4/5	30000

It is of interest to estimate the overall fraction of Magellanic Cloud PN which have WC central stars. As discussed above, helium-shell burning central stars are predicted to decline in luminosity more rapidly than hydrogen-shell burning central stars, and so WR central stars in evolved high-excitation Magellanic Cloud PN may be rather hard to detect. We have therefore confined our comparison to those PN (medium and low excitation) which do not show nebular He II emission lines, implying central star effective temperatures of less than 60000–70000 K. Of the 13 low- and medium-excitation SMC PN, two have WC central stars, while the fraction for LMC PN is three out of 20. Therefore, 15 per cent of SMC and LMC low- and medium-excitation PN have WC central stars. If WC central stars do indeed evolve more rapidly than non-WR central stars, then this may represent a lower limit to the overall fraction of Wolf–Rayet central stars.

A WC-type fraction of 15 per cent is interestingly similar to the fraction of white dwarfs that are hydrogen-deficient (i.e. DB or DO). Fleming, Liebert & Green (1986) have estimated that the fraction of all white dwarfs that are helium-rich is 12 per cent for $T_{\rm eff}$>40000 K and 19 per cent for $T_{\rm eff}$>12000 K. Since WC central stars are clearly helium-rich, our statistics on Magellanic Cloud PN are consistent with a simple scenario whereby the hotter DB and DO white dwarfs evolve from WC central stars, while the remaining central stars evolve into DA white dwarfs. If this is correct, then it implies that the relative fractions of helium- and hydrogen-rich white dwarfs may be determined by events occurring at the end of the AGB phase. Much more complex scenarios for the origin of DB white dwarfs have been proposed previously (see Liebert 1986 for a review).

4 The very-low-excitation nebulae

Among the nebulae included in the current sample are five that were classified as very-low-excitation (VLE) by Sanduleak & Philip (1977). The criteria for this classification (Sanduleak & Stephenson 1972) are that (a) the strength of [O III] 5007 Å be less than that of Hβ, and (b) the strength of [O II] 3727 Å should exceed that of Hβ. The five nebulae in the current sample common to the list of Sanduleak & Philip (1977) are SMC N8 and L302 and LMC N16, N47 and N99. In addition, the nebulae LMC N25 and N101 were found to have [O III] 5007 Å<Hβ, although in both cases the strength of [O II] 3727 Å was only about half that of Hβ.

Morgan (1984) noted that his objective-prism spectrum of SMC L302 appeared anomalous,

since despite satisfying the VLE criteria, strong He II 4686 Å emission was also present. As discussed in the previous section, the central star of this nebulae is a WC8 star, so that strong stellar emission by C III 4650 Å and He II 4686 Å is responsible for the feature seen by Morgan.

Monk (1987) has carried out an H I Zanstra analysis of all of the VLE nebulae in our sample, since they were found to have easily measurable stellar continua. A number of low- and medium-excitation PN in the sample were also analysed in the same way. Monk found that the VLE nebulae SMC N8, LMC N16 and N47 all had stellar luminosities in excess of 15000 $L_\odot$, whereas SMC L302, LMC N99 and N101 were found to have central star luminosities in the range 2200–4800 $L_\odot$, this range being typical of the luminosities derived for the PN central stars in the sample. Monk concluded that the latter three VLE nebulae are planetary nebulae at an early stage in their evolution, whereas SMC N8, LMC N16 and N47 are H II regions powered by Population I stars. The effective temperatures (25000–30000 K) and luminosities (15000–25000 $L_\odot$) found for these three stars are typical of those of early B-type main sequence stars.

Sanduleak & Philip (1977) found that SMC N8, LMC N16 and N47 were spatially resolved on their objective-prism plates, whereas SMC L302 and LMC N99 were stellar in appearance. This is consistent with our classification of the first three as H II regions and the latter two as planetary nebulae. Barlow (1987) derived a nebular mass of 0.27 $M_\odot$ for SMC L302, similar to that found for the other PN in his sample, whereas SMC N8 was found to have a nebular mass of 2.0 $M_\odot$, consistent with it being a Population I H II region.

Finally, a further difference between the three VLE nebulae which we have classified as H II regions and those classified as PN, is that [S II] 6725 Å is very much stronger in the spectra of the former (Table 1). There are probably two factors contributing to this, the first being that the absolute abundance of sulphur is higher in the H II regions than in the PN, and the second being that the nebular electron densities are much lower in the VLE H II regions than in the VLE PN, favouring the efficient excitation of [S II] 6725 Å in the former.

5 Electron densities and electron temperatures

It is possible to calculate the electron temperatures in the O III and N II emission regions and the electron density in the O II emission region [T_e(O III), T_e(N II), and n_e(O II) respectively] using the ratios of the following emission lines:

I(5007+4959 Å)/I(4363 Å) of [O III],
I(6548+6584 Å)/I(5755 Å) of [N II],
I(3729 Å/I(3726 Å) of [O II].

To do this, two statistical equilibrium programs EQUIB, and RATIO (Adams 1983), were used, along with the transition probabilities and collision strengths for O III, N II and O II taken from the references listed in Table 6.

Table 6. References for atomic data.

Ion	Transition Probability	Collision Strength
N II	Nussbaumer & Rusca, 1979.	Seaton, 1975.
O II	Zeippen, 1982.	Pradhan,1976.
O III	Nussbaumer & Storey, 1981.	Baluja, Burke & Kingston, 1980.
Ne III	Mendoza, 1983.	Butler & Mendoza, 1984.
S II	Mendoza & Zeippen, 1982.	Mendoza, 1983.
Ar III	Mendoza & Zeippen, 1983.	Krueger & Czyzak, 1970.
Ar IV	Mendoza & Zeippen, 1982.	Zeippen, Butler, & Le Bourlot, 1987

The resolutions of the spectra reported here are not high enough to resolve the [O II] doublet; but, for 56 PN, data on the [O II] doublet ratio were available from higher resolution AAT IPCS observations (Barlow 1987; Monk, Barlow & Clegg, in preparation). The derived electron densities, n_e(O II), are given in Table 7. For objects not included in this list an electron density of 3500 cm^{-3} was adopted if He II 4686 Å was present in the spectrum, while an electron density of 10^4 cm^{-3} was adopted for those PN not showing He II 4686 Å emission. The T_e and n_e sensitive [O II] intensity ratio, $I(3726+3729)/I(7320+7330)$, was not used in this analysis as it was felt to be too unreliable, due to the generally low signal-to-noise ratios for the latter lines.

An electron temperature, T_e(O III), was calculated from all but 15 of the spectra by deconvolving the [O III] 4363 Å line from Hγ (as described in Section 2.2). The total error in the value of T_e(O III) is determined mainly by the error in the 4363 Å line intensity and more confidence can be placed in the temperatures derived from the medium resolution spectra than those from the low resolution spectra.

The electron temperature of the N^+ region, T_e(N II), was also calculated using lines which suffer some blending, but in this case the overall error is determined mainly by the error in the 5755 Å

Table 7. [O II] electron densities (cm^{-3}) (from Barlow 1987; Monk *et al.* in preparation).

LMC PN	n_e(O II)	SMC PN	n_e(O II)
N1	39500	N1	8950
N24	2700	N2	2850
N25	13500	N4	1800
N28	7300	N5	3900
N39	4800	N6	26600
N60	18800	N8	380
N66	2700	N18	2150
N77F	1600	N29	2750
N78	3300	N38	7100
N97	2400	N40	3550
N101	7600	N42	4900
N102	8200	N43	8800
N104A	4500	N44	4600
N110	13000	N47	36400
N122	2500	N70	9900
N123	9400	N87	6400
N133	66000	L239	3900
N141	7700	L302	930
N153	4600	L305	1900
N170	3300	L536	1900
N178	3900		
N184	3900		
N186A	3750		
N188	2700		
N192	2150		
N199	14400		
N201	4800		
N203	30000		
N208	8700		
N221	2400		
LM1-9	2800		
LM1-27	900		
LM1-61	2050		
S1	2000		
WS12	880		
WS16	2100		

Table 8. Comparison of electron temperatures.

Object	Ion	Medium	Electron Temperature Low	Aller (1983) or Aller *et al.*(1981)	Adopted
LMC N24	[OIII]		12300	11370	12300
LMC N42	[OIII]	15750	16000		15750
LMC N66	[OIII]	15000	17750		15000
	[NII]	11000	11750		11000
LMC N97	[OIII]		20500	19500	20500
	[NII]		11000	11800	11000
LMC N102	[OIII]	23250	19250	19000	23250
	[NII]	12000	13250	14400	12000
LMC N104	[OIII]	13750	12750		13750
LMC N153	[OIII]	13100		13600	13100
LMC N178	[OIII]	11900		13000	11900
LMC N184	[OIII]	12750	13500	14300	12750
	[NII]			11000	11000
LMC LM1-27	[OIII]	11500	15000		11500
LMC LM1-61	[OIII]	14500		15000	14500
SMC N2	[OIII]		13250	12800	13250
SMC N5	[OIII]		14250	13000	14250
SMC N6	[OIII]	14500	15250		14500
SMC N43	[OIII]		13250	12000	13250
SMC N44	[OIII]		12250	12100	12250
SMC N70	[OIII]	10900		10900	10900
SMC N87	[OIII]	13000		12000	13000

line intensity. This line was absent in most spectra, but was clearly present in the spectra of the Type I LMC planetaries N28, N66, N77F, N97, N102, N122 and N181 (see Section 8).

The calculated values of T_e(O III) and T_e(N II) are given in Table 1(a–d), at the bottom of the 'relative line intensity' column for each object. For the 12 PN where no T_e(O III) or T_e(N II) value could be derived, or where the [O III]4363 Å line was very uncertain, a temperature of 10500 K was adopted. Abundances derived assuming such a temperature are indicated by a single colon (:) in Tables 9, 11 and 12.

A check on the accuracy of the derived temperatures is provided by comparing the values obtained from the medium and low resolution spectra with those of Aller *et al.* (1981) and Aller (1983) (see Table 8). The comparison shows reasonable agreement between the datasets, with a spread of ~10 per cent about the mean values. To be self-consistent within this analysis, it was decided to adopt the electron temperatures derived from the medium resolution spectra, where available (final column of Table 8), and again these adopted values are within ~10 per cent of the mean value. This scatter of 10 per cent, though, is probably a lower limit on the overall accuracy, as it is derived from a comparison between the brighter objects in the sample.

6 Helium abundances

Following the work of Peimbert & Torres-Peimbert (1971) and Brocklehurst (1972), it had generally been assumed when calculating helium abundances for PN that the He I 4471, 5876, and 6678 Å lines were purely due to radiative recombination. However, Ferland (1986) pointed out that the calculations of Berrington *et al.* (1985) implied that collisional excitations from the metastable 2^3S state are not negligible for conditions appropriate to PN, and that the observed

intensities of the He I 4471, 5876, and 6678 Å lines will be partly due to recombination and partly to radiative transitions following collisional excitation from the 2^3S level to the $n=3$, $n=4$, and higher levels.

Based on the 11 state (up to $n=3$) calculations of Berrington *et al.* (1985), Ferland (1986) was able to estimate, as a function of electron temperature and density, the ratio of the 'collisional' to 'recombination' contributions to the intensity of the He I 4471, 5876, and 6678 Å lines. A recent 19 state calculation by Berrington & Kingston (1987) which includes the $n=4$ levels has shown that the earlier 11 state calculation significantly overestimated the collisional rates to the $n=3$ levels from 2^3S, so, in a similar manner to Ferland (1986), Clegg (1987) has derived the following empirical formulae to estimate the collisional contribution to the intensities of the He I 4471, 5876 and 6678 Å lines.

$$\frac{I(4471)_{\rm coll}}{I(4471)_{\rm rec}}=\frac{6.11\,t^{0.02}\,{\rm e}^{-4.544}/t}{1+(3110\,t^{-0.51}/n_e)}$$

$$\frac{I(5876)_{\rm coll}}{I(5876)_{\rm rec}}=\frac{(7.12t^{0.14}\,{\rm e}^{-3.776/t}+1.47\,t^{-0.28}\,{\rm e}^{-4.544/t})}{1+(3110\,t^{-0.51}/n_e)}$$

$$\frac{I(6678)_{\rm coll}}{I(6678)_{\rm rec}}=\frac{(3.27\,t^{-0.41}\,{\rm e}^{-3.777/t}+0.49t^{-0.52}\,{\rm e}^{-4.544/t})}{1+(3110\,t^{-0.51}/n_e)}.$$

These equations include estimates for cascades from the $n=4$ level that contribute to the He I 5876 and 6678 Å lines, but take no account of photoionization from the lower levels.

The collisional contribution to the He I recombination lines was found to be largest for He I 5876 Å (contributing an average of 18.5 per cent of the total flux in this line, versus 7.8 per cent of the 4471 Å flux, and 8.5 per cent of the 6678 Å flux, for the case of the LMC PN).

After subtracting the collisional contributions to the He I line fluxes that are predicted by the above equations, the He II 4686 Å fluxes and the corrected He I line fluxes were used to derive the He^{2+} and He^{+} abundances relative to H^{+}, from the equation

$$\frac{N({\rm He^{m+}})}{N({\rm H^+})}=\frac{I(\lambda)}{I({\rm H}\beta)}\,\frac{\alpha^{\rm eff}_{{\rm H}\beta}[n_e,\,T_e({\rm H^+})]}{\alpha^{\rm eff}_{{\rm He^{m+}}}[n_e,\,T_e({\rm He^{m+}})]}\,\frac{\lambda}{4861}.$$

The recombination coefficients, $\alpha_{{\rm H}\beta}$ and $\alpha_{\rm He}$, were taken from Brocklehurst (1971, 1972) (which agree to within 1 per cent with the more recent calculations of Hummer & Storey 1987) and the [O III] electron temperatures from Table 1(a–d) were adopted for $T_e({\rm H^+})$ and $T_e({\rm He^{m+}})$.

The ionic abundances derived from the He I 6678, 4471 and 5876 Å lines have significantly different errors associated with them, owing to the different intrinsic intensities of the lines, and to the differing detector sensitivity in the regions where they fell (see Section 2.3). The instrumental sensitivity is a function of wavelength, with the highest sensitivity at the central wavelengths and a gradual fall off in sensitivity towards the detector edges. The effects of this sensitivity variation are small for the low resolution spectra, since the three He I lines all fall in the central zone of the detector. For the medium resolution spectra, however, the 4471 and 6678 Å lines fell closer to the outer, less sensitive zones of the detector.

It was decided, therefore, to base overall He^{+} abundances on different procedures for the medium and low resolution spectra. The adopted He^{+} abundance for the low resolution spectra is the weighted (1:3:1) mean of the abundances derived from the 4471, 5876 and 6678 Å lines respectively, since the instrumental sensitivity variations can be ignored, and the weighting applied is directly proportional to the intrinsic intensities of the three lines. For the medium

resolution spectra, the He^+ abundance was derived from the 5876 Å line alone, due to its much higher signal-to-noise ratio arising from its placement in the highest sensitivity region of the detector.

Table 9(a) summarizes the ionic helium abundances derived for the eight PN having both medium- and low-resolution spectra, while Tables 9(b) and (c) summarize the ionic helium abundances derived for the rest of the LMC and SMC PN. Entries labelled with an 'a' are derived using the results of Barlow (1987), and those designated with ':' are derived using an assumed T_e of 10 500 K. The last column of Table 9(a–c) lists the overall He/H abundance ratio found for each nebula.

Table 10 presents the mean He/H ratios (by number) derived for 13 SMC PN and for 32 LMC PN. Type I PN (Section 8) and low-excitation PN [those with $I(5007)<4\times I(H\beta)$] were excluded from these means – a Zanstra analysis of the central stars of the latter by Monk (1987) showed that their effective temperatures are not sufficiently high to fully ionize helium in the surrounding nebulae. Nebulae with colons following their derived helium abundances were also excluded from the means given in Table 10.

The first row in Table 10 gives the He/H ratios obtained when no correction is made for collisional contributions to the He I lines, while the second row gives the ratios after correction for collisional excitation. For comparison, Table 10 also presents the mean He/H ratios for 3 SMC H II regions and 4 LMC H II regions discussed by Dufour, Shields & Talbot (1982), both before (first row) and after (second row) correction for collisional excitation of the He I lines (the electron temperatures and densities adopted by Dufour *et al.* were used for this). Inspection of Table 10 shows that the effect of collisions on the observed He I line intensities is very much

Table 9(a). Comparison of ionic helium abundances by number relative to H^+, for PN with both medium (M) and low (L) resolution spectra.

OBJECT	Res^n.	He^+ (6678)	He^+ (4471)	He^+ (5876)	He^+ (Adopt)	He^{2+} (4686)	He/H
LMC							
N42	M	0.104		0.079	0.079		0.079
N42	L	0.088	0.058	0.058	0.066		0.066
N66 (Ty I)	M			0.046	0.046	0.053	0.099
N66 (Ty I)	L			0.032	0.032	0.058	0.090
N102 (Ty I)	M		0.073	0.047	0.047	0.072	0.119
N102 (Ty I)	L	0.082	0.068	0.044	0.053	0.064	0.117
N104A*	M			0.057	0.057	0.034	0.091
N104A	L	0.075		0.051	0.057	0.033	0.090
N184	M	0.101	0.069	0.064	0.064	0.039	0.103
N184	L	0.057	0.071	0.054	0.055	0.035	0.090
LM1-27	M			0.074	0.074	0.010	0.084
LM1-27	L	0.093		0.082	0.084	0.012	0.096
SMC							
N1 (LE)	M	0.087:	0.109:	0.055:	0.055:		0.055:
N1 (LE)	L	0.076:	0.059:	0.059:	0.064:		0.064:
N6	M	0.114	0.114	0.080	0.080		0.080
N6	L	0.116	0.076	0.067	0.079		0.079

Table 9(b). Ionic helium abundances for LMC PN, by number relative to H^+.

OBJECT	Res$^{n.}$	He^+ (6678)	He^+ (4471)	He^+ (5876)	He^+ (Adopt)	He^{2+} (4686)	He/H
N1 (LE)	M	0.089:		0.083:	0.083:		0.083:
N24	L		0.098	0.078	0.078		0.078
N25 (VLE)	M			0.031:	0.031:		0.031:
N28 (Ty I)	L	0.051	0.051	0.051	0.051	0.040	0.091
N39	L	0.061	0.033	0.070	0.068	0.016	0.084
N52	M	0.104	0.093	0.070	0.070	0.020	0.090
N60	M	0.080	0.085	0.081	0.081		0.081
N77F (Ty I)	M			0.041	0.041	0.060	0.101
N78	M	0.110:	0.140:	0.097:	0.097:		0.097:
N97 (Ty I)	L		0.056	0.058	0.058	0.055	0.113
N99 (VLE)	M			0.013:	0.013:		0.013:
N101 (VLE)	M			0.008:	0.008:		0.008:
N107*	L			0.085::	0.085::	0.033	0.118:
N110	M	0.127	0.089	0.094	0.094		0.094
N122 (Ty I)	M		0.096	0.093	0.093	0.036	0.129
N123	M	0.075	0.088	0.082	0.082		0.082
N124	M	0.087	0.068	0.065	0.065	0.020	0.085
N125	M	0.122	0.081	0.088	0.088		0.088
N133	M	0.065	0.080	0.072	0.072		0.072
N141	M	0.086	0.085	0.084	0.084		0.084
N151	M	0.115	0.092	0.084	0.084		0.084
N153	M	0.067	0.075	0.058	0.058	0.026	0.084
N170	M	0.117	0.081	0.065	0.065	0.027	0.092
N178	M	0.058	0.055	0.076	0.076	0.008	0.084
N181 (Ty I)	M		0.108	0.059	0.059	0.048	0.107
N182	M	0.080	0.077	0.088	0.088		0.088
N186A	L	0.040	0.051	0.072	0.064	0.023	0.087
N188	L	0.053		0.048	0.049	0.030	0.079
N192	L	0.063		0.039	0.045	0.053	0.098
N199 (LE)	M	0.060:	0.083:	0.042:	0.042:		0.042:
N201 (Ty I)	M	0.083	0.052	0.066	0.066	0.022	0.088
N203	M	0.080		0.094	0.094		0.094
N207 (Ty I)	M	0.082	0.098	0.065	0.065	0.037	0.102
N208	M	0.072	0.074	0.070	0.070	0.021	0.091
N209	M	0.103		0.075	0.075	0.020	0.095
N211	M	0.088	0.078	0.079	0.079		0.079
N212	M			0.098::	0.098::		0.098:
N221 (Ty I)	M	0.050	0.071	0.075	0.075	0.017	0.092
LM1-9	L	0.082		0.056	0.062	0.026	0.088
LM1-61	M		0.042	0.025	0.025	0.057	0.082
LM1-62	M	0.066	0.075	0.081	0.081	0.013	0.094
S1 (LE)	M			0.090:	0.090:		0.090
WS12	L		0.064	0.063	0.063	0.016	0.079
WS16	L			0.069	0.069	0.046	0.115

Table 9(c). Ionic helium abundances for SMC PN, by number relative to H^+.

OBJECT	Res^{n}.	He^+ (6678)	He^+ (4471)	He^+ (5876)	He^+ (Adopt)	He^{2+} (4686)	He/H
N2	L		0.037	0.061	0.061	0.022	0.083
N4	M		0.094b		0.094	0.007	0.101
N5	L	0.083	0.077	0.050	0.058	0.035	0.093
N7	L	0.110	0.076	0.074	0.083		0.083
N18	L			0.070	0.070		0.070
N29 (LE)	L			0.067:	0.067:		0.067:
N38	L	0.082	0.066	0.070	0.073		0.073
N40	L			0.051	0.051	0.029	0.080
N42 (LE)	L			0.067:	0.067:		0.067:
N43	L	0.053	0.105	0.081	0.074		0.074
N44	L	0.054	0.114	0.077	0.071		0.071
N47 (LE)	L	0.067:	0.088:	0.077:	0.075:		0.075:
N70	M	0.062	0.156	0.076	0.076		0.076
N87	M	0.093	0.058	0.091	0.091		0.091
L66*	M		0.046a		0.046	0.059	0.105
L239	M	0.078	0.070	0.063	0.063	0.042	0.105
L305 (Ty I)*	M			0.063	0.063	0.038	0.103
L536 (Ty I)	M	0.144		0.090	0.090	0.051	0.141

Table 10. Helium abundances in PN and H II regions in the Magellanic Clouds.

	Mean He/H number ratios			
	SMC PN	SMC H II	LMC PN	LMC H II
Sample size	13	3	32	4
He/H before correction for He I collisional excitation	0.100 ± 0.010	0.083 ± 0.004	0.105 ± 0.010	0.083 ± 0.004
He/H after correction for He I collisional excitation	0.083 ± 0.011	0.081 ± 0.003	0.087 ± 0.008	0.082 ± 0.004
Corrected helium mass fraction, Y	0.249 ± 0.025	0.245 ± 0.007	0.258 ± 0.015	0.247 ± 0.009

smaller for the H II regions than for the PN, due to the lower temperatures and densities characteristic of the former.

Table 10 shows that, when no correction is made for He I collisional excitation, the mean He/H ratio found for PN is significantly larger than for H II regions in the same galaxy. A similar enhancement of helium, relative to H II regions, was found in the past for PN in the Milky Way (e.g. Torres-Peimbert & Peimbert 1977; Aller & Czyzak 1983a). One suggested explanation (Kaler 1978) was that helium-rich products of hydrogen-burning had been dredged to the surfaces of the progenitor stars. However, the results in the second row of Table 10 and in Table 14 show that, once the corrections for He I collisional excitation are made, the He/H ratios for PN are only very slightly larger than those for H II regions in the same galaxy, and are the same within one standard deviation. Clegg (1987) found a similar result when comparing only Galactic PN and H II regions.

The mean helium mass fraction, Y, after correction for collisional excitation of He I, is given in

the last row of Table 10, for PN and H II regions in the SMC and LMC. We find mean Y values of 0.249 and 0.258 for the SMC and LMC PN respectively, and nominal excesses over the H II region values of $\Delta Y=0.00\pm0.02$ and 0.01 ± 0.02. Peimbert & Torres-Peimbert (1987) presented evidence that in planetary nebulae the population of metastable (2^3S) helium is only about half the predicted value (Clegg 1987). This would yield mean Y values of 0.267 and 0.276 for the SMC and LMC PN, respectively, and nominal 'excesses' over the H II region values of $\Delta Y=0.02\pm0.02$ and 0.03 ± 0.02 for these galaxies.

All of the above results are consistent, within the uncertainties, with the predicted enrichment of helium for metal poor stars experiencing a first dredge-up phase, $\Delta Y=0.01$–0.02 (Renzini & Voli 1981). The Magellanic Cloud PN and H II region helium abundances are actually indistinguishable in this work; at present, a single value, $Y=0.25\pm0.02$, seems to be consistent with all of the data on PN and H II regions in both of these galaxies. The predicted enhancement of the abundance of helium for the first dredge-up is too small to test observationally without extremely accurate (~1–2 per cent) helium abundances. The implications of our results for the predicted helium enrichment by the third dredge-up ($\Delta Y=0.03$–0.05; Renzini & Voli 1981) will be discussed in a later paper, on carbon abundances for Magellanic Cloud planetary nebulae derived from *IUE* spectra.

7 Ionic abundances for N, O, Ne and Ar

The intensities given in Table 1 for the collisionally excited lines of [N II] 6548, 6584 Å, [O II] 3727 Å, [O III] 4959, 5007 Å, [Ne III] 3868 Å, [Ar III] 7135 Å, [Ar IV] 4740 Å, and [S II] 6717, 6731 Å were used to derive the abundances (relative to H^+) of N^+, O^+, O^{2+}, Ne^{2+}, Ar^{2+}, Ar^{3+}, and S^+, using the multilevel statistical equilibrium code EQUIB (Adams 1983).

When only T_e (O III) was available it was adopted for all ions; if T_e (N II) was also available it was adopted for the O^+, N^+ and S^+ ions. The sources for the atomic parameters used are listed in Table 6, while the adopted electron densities are as given in Table 7 (see Section 5).

The calculation of elemental abundances is limited by the absence of optical lines from the higher ionic species of most elements. However, it is possible to make an empirical correction to the lower stage ionic abundances in order to determine the overall elemental abundances (Peimbert & Torres-Peimbert 1971). Barker (1983) has discussed ionization correction procedures for He, O, N, Ne, Ar and S, and has found a reasonable agreement between element abundances calculated from optical lines only (using the necessary ionization correction factors, ICFs) and those derived using *IUE* ultraviolet observations of lines from higher ionic stages to supplement the optical data.

The ionization correction procedures for He, O, N, Ne and Ar used by Torres-Peimbert & Peimbert (1977) and Barker (1983, 1980) are adopted here:

$$\mathrm{He/H}=(\mathrm{He^+/H^+})+(\mathrm{He^{2+}/H^+})$$
$$\mathrm{O/H}=[(\mathrm{O^+/H^+})+(\mathrm{O^{2+}/H^+})]\times\mathrm{ICF(O)}$$
$$\mathrm{N/H}=(\mathrm{N^+/H^+})\times\mathrm{ICF(N)}$$
$$\mathrm{Ne/H}=(\mathrm{Ne^{2+}/H^+})\times\mathrm{ICF(Ne)}$$
$$\mathrm{Ar/H}=1.5\times(\mathrm{Ar^{2+}/H^+}),$$

where

$$\mathrm{ICF(O)}=(\mathrm{He^+}+\mathrm{He^{2+}})/\mathrm{He^+}$$
$$\mathrm{ICF(N)}=\mathrm{O/O^+}$$
$$\mathrm{ICF(Ne)}=\mathrm{O/O^{2+}}.$$

The absence, or blending, of the 6312 Å [S III] line meant that no correction procedures could

be applied for sulphur and therefore no total sulphur abundances could be derived from the S^+ ionic abundances. The Ar^{2+} and total Ar abundances could only be derived from the low-resolution spectra, since the wavelength coverage of the medium resolution spectra did not extend to [Ar III] 7135 Å.

The ionic and elemental abundances derived by the procedures outlined above are presented in Tables 11(a) and 12(a) for the eight objects with both medium and low resolution spectra. In Table 11(b) and (c) we present the ionic abundances derived for of the objects with only a low resolution or a medium resolution spectrum and in Tables 12(b) and (c) we present the overall elemental abundances for all LMC and SMC objects in this survey. In these tables entries labelled 'a' are derived from the results of Barlow (1987), and those designated ':' are derived from an assumed T_e of 10500 K.

From an inspection of Tables 9(a), 11(a) and 12(a) it is possible to estimate the effects of the calibration corrections applied to the medium resolution [O II] 3727 Å and [Ne III] 3868 Å line intensities (see Section 2.3). The calibration correction to the [O II] line will increase the derived oxygen abundance of each object by varying amounts depending on the contribution to the total oxygen abundance made by the O^+ ion relative to that by the O^{2+} ion. In two cases, LMC N99 and LMC N101, the O^+ ions make the dominant contribution and the abundance will increase in almost direct proportion to O^+. For all other objects the increase in the derived oxygen abundance due to the corrections (discussed in Section 2.3) is less than 33 per cent, and for the majority of these objects it is less than 6 per cent.

A comparison of the O^+ abundances derived from the low and medium resolution spectra

Table 11(a). Comparison of ionic abundances by number relative to H^+, for PN with both medium (M) and low (L) resolution spectra.

OBJECT	Res$^{n.}$	N^+ (6584)	O^+ (3727)	O^{2+} (5007)	Ne^{2+} (3868)	S^+ (6717/31)	Ar^{2+} (7135)	Ar^{3+} (4740)
LMC								
N42	M	4.9(-6)	< 1.8(-5)	1.4(-4)	< 2.1(-5)	1.7(-7)		
N42	L	2.6(-6)	1.6(-5)	1.2(-4)	2.0(-5)	2.3(-7)	2.8(-7)	
N66 (Ty I)	M	1.8(-5)	2.2(-5)a	1.1(-4)	2.1(-5)	3.7(-7)		6.1(-7)
N66 (Ty I)	L	1.9(-5)	2.7(-5)	9.4(-5)	1.7(-5)	5.3(-7)	4.4(-7)	1.2(-6)
N102 (Ty I)	M	4.6(-5)	2.2(-5)	5.4(-5)	7.9(-6)	1.1(-6)		5.8(-7)
N102 (Ty I)	L	4.7(-5)	2.7(-5)	4.7(-5)	8.6(-6)	1.0(-6)	3.8(-7)	5.1(-7)
N104A*	M	7.9(-6)	< 3.9(-5)	2.2(-4)	2.7(-5)	3.9(-7)		
N104A	L	6.3(-6)	3.3(-5)	1.7(-4)	2.4(-5)	3.7(-7)	4.5(-7)	
N184	M	4.1(-6)	2.3(-5)	2.3(-4)	3.7(-5)	2.3(-7)		
N184	L	2.3(-6)	2.9(-5)	2.0(-4)	2.8(-5)	1.9(-7)	4.1(-7)	2.9(-7)
LM1-27	M	8.5(-6)	2.6(-5)	2.9(-4)	4.1(-5)	4.8(-7)		
LM1-27	L	9.3(-6)	4.3(-5)	2.7(-4)	5.0(-5)	4.8(-7)	9.7(-7)	2.3(-6)
SMC								
N1 (LE)	M	3.0(-6):	2.5(-5):	6.2(-5):	< 1.1(-5):			
N1 (LE)	L	2.9(-6):	2.4(-5):	5.9(-5):	< 4.8(-6):		3.5(-7):	
N6	M	5.4(-6)	1.8(-5)a	9.9(-5)	1.6(-5)a			
N6	L	6.2(-6)	1.8(-5)a	1.0(-4)	9.1(-6)·	2.1(-7)	3.0(-7)	

Table 11(b). Ionic abundances for LMC PN, by number relative to H^+.

OBJECT	Res^n.	N^+ (6584)	O^+ (3727)	O^{2+} (5007)	Ne^{2+} (3868)	S^+ (6717/31)	Ar^{2+} (7135)	Ar^{3+} (4740)
N1 (LE)	M	9.8(-7):	< 3.8(-5):	1.3(-4):	< 1.9(-5):			
N24	L		6.8(-6)	1.5(-4)	1.7(-5)		5.2(-7)	
N25 (VLE)	M	9.4(-6):	4.6(-5):	1.5(-5):	< 1.3(-5):			
N28 (Ty I)	L	3.0(-5)	6.1(-5)	1.6(-4)	1.9(-5)	5.8(-7)	5.5(-7)	5.8(-7)
N39	L	7.1(-7)	4.0(-6)	1.5(-4)	2.0(-5)	6.6(-8)	2.3(-7)	
N52	M	2.1(-7)	< 9.4(-6)	2.7(-4)	3.0(-5)			6.3(-7)
N60	M	2.4(-6)	< 3.1(-5)	1.8(-4)	2.7(-5)	1.5(-7)		
N77F (Ty I)	M	4.8(-5)	4.8(-5)	1.3(-4)	1.5(-5)	2.4(-7)		
N78	M	3.3(-6):	1.3(-5):	1.7(-4):	2.6(-5):	9.1(-8):		
N97 (Ty I)	L	8.0(-5)	3.9(-5)	5.7(-5)	1.1(-5)	1.2(-6)	3.6(-7)	3.3(-7)
N99 (VLE)	M	2.6(-5):	5.8(-4):	2.2(-6):	9.7(-6)::			
N101 (VLE)	M	1.6(-5):	3.5(-5):	7.0(-7):	2.0(-5):			
N107*	L	2.5(-6)	< 5.4(-6)	1.8(-4)	3.2(-5)		5.6(-7)	
N110	M	8.0(-6)	6.4(-5)	3.7(-4)	5.7(-5)	3.0(-7)		
N122 (Ty I)	M	2.3(-5)	8.2(-6)	1.3(-4)	2.9(-5)	2.2(-7)		7.2(-7)
N123	M	3.8(-6)	2.2(-5)	1.8(-4)	2.2(-5)	1.5(-7)		
N124	M	2.2(-6)	7.3(-6)	2.5(-4)	2.1(-5)	1.1(-7)		2.7(-7)
N125	M	1.9(-6)	1.7(-5)::	2.1(-4)	1.7(-5)::	1.6(-7)		
N133	M	1.0(-6)	1.0(-5)a	1.4(-4)	1.4(-5)a			
N141	M	3.1(-6)	1.3(-5)	2.8(-4)	2.6(-5)	1.5(-7)		
N151	M	2.9(-6)	< 2.0(-5)	2.2(-4)	3.5(-5)			
N153	M	4.2(-6)	1.3(-5)	2.3(-4)	3.1(-5)	1.3(-7)		4.0(-7)
N170	M	6.2(-6)	1.8(-5)	3.0(-4)	3.8(-5)	2.7(-7)		6.4(-7)
N178	M	3.7(-6)	1.8(-5)	2.9(-4)	3.6(-5)	1.3(-7)		3.3(-7)
N181 (Ty I)	M	2.5(-4)	1.6(-4)	6.9(-5)	2.6(-5)	3.6(-6)		
N182	M	2.4(-6)	2.1(-5)	2.1(-4)	2.9(-5)			
N186A	L	4.6(-6)	3.5(-5)	2.9(-4)	6.1(-5)	2.5(-7)	6.9(-7)	
N188	L	6.5(-6)	3.1(-5)	2.1(-4)	2.3(-5)	4.1(-7)	5.6(-7)	5.2(-7)
N192	L	1.4(-6)	1.3(-5)	1.6(-4)	2.1(-5)	1.7(-7)	3.8(-7)	6.4(-7)
N199 (LE)	M	1.5(-5):	5.3(-5):	4.6(-5):	< 5.4(-6):	1.4(-7):		
N201 (Ty I)	M	2.5(-6)	4.8(-6)	1.2(-4)	1.3(-5)	1.3(-7)		4.6(-7)
N203	M	5.8(-6)	1.4(-4)a	3.0(-4)	3.9(-5)	7.5(-7)		
N207 (Ty I)	M	8.7(-6)	2.0(-5)	2.5(-4)	3.8(-5)	3.5(-7)		
N208	M	5.7(-6)	2.6(-5)	2.8(-4)	4.5(-5)	2.7(-7)		3.2(-7)
N209	M	4.0(-6)	1.4(-5)	2.8(-4)	3.9(-5)	1.9(-7)		5.1(-7)
N211	M	1.2(-6)	< 1.2(-5)	1.8(-4)	1.9(-5)::	1.3(-7)		3.1(-7)
N212	M	9.0(-7)	1.6(-5)	1.2(-4)	1.1(-5)::	9.0(-8)		
N221 (Ty I)	M	1.7(-5)	1.7(-5)	3.2(-4)	2.5(-5)	2.6(-7)		2.3(-7)
LM1-9	L	1.0(-6)	7.5(-6)::	1.4(-4)	1.6(-5)	7.8(-8)	2.4(-7)	4.7(-7)
LM1-61	M	5.2(-7)	2.8(-6)a	1.2(-4)	1.3(-5)			4.7(-7)
LM1-62	M	3.3(-6)	9.5(-6)	2.6(-4)	4.1(-5)	1.2(-7)		2.8(-7)
S1 (LE)	M	4.3(-6):	8.2(-5):	8.5(-5):	< 2.7(-5):			
WS12	L	4.0(-6)	2.3(-5)	2.6(-4)	4.0(-5)	8.7(-8)	5.8(-7)	
WS16	L	1.3(-5)	6.2(-5)	2.0(-4)	3.6(-5)	6.4(-7)	1.1(-6)	
N16 (VLE)	M	6.9(-6):	5.6(-4):	3.2(-6)::		2.3(-6):		
N47 (VLE)	M	7.5(-6):	3.0(-4):			3.5(-6):		

Table 11(c). Ionic abundances for SMC PN, by number relative to H^+.

OBJECT	Res^n.	N^+ (6584)	O^+ (3727)	O^{2+} (5007)	Ne^{2+} (3868)	S^+ (6717/31)	Ar^{2+} (7135)	Ar^{3+} (4740)
N2	L		1.5(-6)	1.3(-4)	1.5(-5)	5.5(-8)	2.1(-7)	
N4	M	4.5(-7)	3.3(-6)a	1.9(-4)	1.6(-5)a			
N5	L	2.1(-6)	1.1(-5)	1.3(-4)	1.7(-5)	1.5(-7)	2.4(-7)	
N7	L		4.1(-6)	1.1(-4)	9.3(-6)		1.3(-7)	
N18	L		4.0(-6)::	2.0(-4)	1.9(-5)	1.4(-7)	4.4(-7)	
N29 (LE)	L		9.1(-5):	9.6(-5):	< 3.6(-5):	2.4(-7):	7.5(-7):	
N38	L		1.1(-5)	1.4(-4)	2.2(-5)		2.0(-7)	
N40	L		1.5(-5)	1.8(-4)	3.2(-5)		2.7(-7)	
N42 (LE)	L	2.6(-6):	7.8(-5):	4.9(-5):	< 2.4(-5):			
N43	L		3.6(-6)	9.6(-5)	1.5(-5)	2.7(-8)	2.0(-7)	
N44	L		6.4(-6)	1.7(-4)	3.2(-5)		2.3(-7)	
N47 (LE)	L	2.9(-6):	1.0(-4):	9.3(-5):	1.7(-5):		5.6(-7):	
N70	M	2.5(-6)	5.5(-5)a	1.3(-4)	1.5(-5)a	9.0(-8)		
N87	M	4.6(-7)	4.5(-6)a	1.0(-4)	9.9(-6)a			
L66*	M	4.5(-6)	2.8(-5)a	2.5(-4)	2.6(-5)a			
L239	M	8.1(-7)	7.7(-6)a	1.7(-4)	2.1(-5)			
L302 (VLE)	M	1.8(-5):	9.6(-5):	2.0(-5):				
L305 (Ty I)*	M	5.8(-6)	1.6(-6)a	4.0(-5)	8.7(-6)a			
L536 (Ty I)	M	9.4(-6)	2.2(-6)a	1.2(-5)	4.4(-6)a	1.2(-7)		2.2(-7)
N8 (VLE)	L	7.2(-6):	1.6(-4):			7.0(-7):		

(Table 11a) shows agreement to within 30 per cent for all objects except LMC LM1–27. For this case, the [O II] 3727 Å line intensity from the low-resolution spectra is probably the more reliable, and the low resolution values of the O^+ ionic abundance should be adopted. A comparison of the overall oxygen abundances (Table 12a) shows better agreement (within 20 per cent), reflecting the small effect that the uncertainty in O^+ abundance has on the oxygen abundance for the majority of the PN studied.

Owing to the placement of [Ne III] 3868 Å on a lower sensitivity region of the detector, neon abundances derived from the medium resolution spectra are significantly less reliable than those derived from the low resolution spectra. Since O^{2+} generally dominates over O^+, the ICF for Ne, and thus the derived Ne abundances, is not very sensitive to uncertainties in the O^+ abundance derived from [O II] 3727 Å. From the comparison of ionic abundances (Table 11a) it can be seen that there is agreement between the medium and low resolution spectra for Ne^{2+}/H^+ to within 30 per cent for all objects, except for SMC N1 where upper limits for the [Ne III] 3868 Å line intensity in both spectra are given. The agreement between the neon abundances derived from low and medium resolution spectra (Table 12a) is generally within 25 per cent.

The total nitrogen abundances are inversely proportional to the [O II] 3727 Å line intensity, since it affects the nitrogen ICF linearly (the nitrogen ICFs of the two VLE objects LMC N99 and LMC N101 are unaltered). A comparison of N^+ ionic abundances derived from low and medium resolution spectra (Table 11a) shows reasonable agreement, although the values derived from the medium-resolution data are less uncertain, because of better resolution of the Hα [N II] blend, and should therefore be adopted.

For most cases, a comparison of the nitrogen abundances derived from low- and medium-resolution spectra (Table 11a) shows reasonable agreement, except where the [O II] 3727 Å line is either 'very uncertain' (designated ::) or an upper limit, which then leads to a very uncertain, or lower limit for the nitrogen ICF. For LMC N184, however, the two O^+ ionic abundances are in

Table 12(a). Comparison of elemental abundances by number relative to hydrogen, for PN with both medium (M) and low (L) resolution spectra.

OBJECT	Res^n	He	N	O	Ne	Ar
LMC						
N42	M	0.079	4.3(-5)	1.6(-4)	< 2.4(-5)	
N42	L	0.066	2.1(-5)	1.3(-4)	2.3(-5)	4.2(-7)
Adopted		0.073	4.0(-5)c	1.3(-4)	2.3(-5)	4.2(-7)
N66 (Ty I)	M	0.099	2.3(-4)b	2.8(-4)	5.5(-5)	
N66 (Ty I)	L	0.090	2.4(-4)	3.4(-4)	6.1(-5)	6.6(-7)
Adopted		0.094	2.3(-4)	3.2(-4)	5.8(-5)	6.6(-7)
N102 (Ty I)	M	0.119	4.0(-4)	1.9(-4)	2.8(-5)	
N102 (Ty I)	L	0.117	2.8(-4)	1.6(-4)	3.0(-5)	5.8(-7)
Adopted		0.118	3.4(-4)	1.8(-4)	2.9(-5)	5.8(-7)
N104A*	M	0.091	8.2(-5)	4.1(-4)	5.0(-5)	
N104A	L	0.090	6.2(-5)	3.2(-4)	4.5(-5)	6.7(-7)
Adopted		0.091	7.7(-5)c	3.2(-4)	4.8(-5)	6.7(-7)
N184	M	0.103	7.4(-5)	4.1(-4)	6.6(-5)	
N184	L	0.090	3.0(-5)	3.7(-4)	5.2(-5)	6.2(-7)
Adopted		0.096	7.4(-5)	3.8(-4)	5.9(-5)	6.2(-7)
LM1-27	M	0.084	1.1(-4)	3.6(-4)	5.2(-5)	
LM1-27	L	0.096	7.7(-5)	3.6(-4)	6.7(-5)	1.5(-6)
Adopted		0.090	9.4(-5)	3.6(-4)	6.0(-5)	1.5(-6)
SMC						
N1 (LE)	M	0.055:	1.0(-5):	8.8(-5):	< 1.5(-5):	
N1 (LE)	L	0.064:	1.0(-5):	8.3(-5):	< 6.7(-6):	5.2(-7):
Adopted		0.060:	1.0(-5):	8.6(-5):	< 6.7(-6):	5.2(-7):
N6	M	0.080	3.5(-5)	1.2(-4)	1.9(-5)a	
N6	L	0.079	4.2(-5)	1.2(-4)	1.1(-5)	4.5(-7)
Adopted		0.080	3.9(-5)	1.2(-4)	1.5(-5)	4.5(-7)

good agreement and it is the poor N^+ abundance derived from the low resolution data that has caused the discrepancy between the elemental abundances. When both low- and medium-resolution spectra exist, the nitrogen ICF calculated using the low-resolution [O II] 3727 Å line intensity, together with the N^+ ionic abundance derived from the medium-resolution data, yield the best overall value for the nitrogen abundance. Such nitrogen abundances are labelled 'c' in Tables 11 and 12, whilst entries labelled 'b' have a nitrogen ICF derived using the Barlow (1987) O II data.

The third line in Table 12(a) gives the adopted abundance of each element for PN having both low- and medium-resolution spectra, derived from the mean of the low- and medium-resolution values where appropriate, or in the cases where there was a definite difference in quality between the two datasets, from the better data as outlined above.

8 Type I PN

Type I planetary nebulae have been defined by Peimbert & Torres-Peimbert (1983; PTP83) as those Galactic planetary nebulae which have significantly enhanced helium and nitrogen abun-

Table 12(b). Elemental abundances for LMC PN, by number relative to hydrogen.

OBJECT	He	N	O	Ne	Ar
N1 (LE)	0.083:	> 4.3(-6):	1.6(-4):	< 2.5(-5):	
N24	0.078		1.6(-4)	1.8(-5)	7.8(-7)
N25 (VLE)	0.031:	1.2(-5):	6.1(-5):	< 5.3(-5):	
N28 (Ty I)	0.091	2.0(-4)	3.9(-4)	4.7(-5)	8.3(-7)
N39	0.084	3.3(-5)	1.9(-4)	2.5(-5)	3.4(-7)
N42	0.073	4.0(-5)c	1.3(-4)	2.3(-5)	4.2(-7)
N52	0.090	> 8.2(-6)	3.6(-4)	4.0(-5)	
N60	0.081	> 1.6(-5)	2.1(-4)	3.1(-5)	
N66 (Ty I)	0.094	2.3(-4)	3.2(-4)	5.8(-5)	6.6(-7)
N77F (Ty I)	0.101	4.4(-4)	4.4(-4)	5.0(-5)	
N78	0.097:	4.5(-5):	1.8(-4):	2.8(-5):	
N97 (Ty I)	0.113	3.8(-4)	1.9(-4)	3.5(-5)	5.3(-7)
N99 (VLE)	0.013:	2.6(-5):	5.8(-4):		
N101 (VLE)	0.008:	1.6(-5):	3.5(-5):		
N102 (Ty I)	0.118	3.4(-4)	1.8(-4)	2.9(-5)	5.8(-7)
N104A*	0.091	7.7(-5)c	3.2(-4)	4.8(-5)	6.7(-7)
N107*	0.118::	> 1.2(-4)	2.6(-4)	4.6(-5)	8.4(-7)
N110	0.094	5.5(-5)	4.4(-4)	6.6(-5)	
N122 (Ty I)	0.129	5.5(-4)	2.0(-4)	4.3(-5)	
N123	0.082	3.5(-5)	2.1(-4)	2.4(-5)	
N124	0.085	9.8(-5)	3.3(-4)	2.9(-5)	
N125	0.088	2.5(-5)	2.2(-4)	1.8(-5)::	
N133	0.072	1.4(-5)	1.5(-4)	1.5(-5)a	
N141	0.084	7.0(-5)	2.9(-4)	2.7(-5)	
N151	0.084	3.5(-5)	2.4(-4)	3.8(-5)	
N153	0.084	1.2(-4)	3.5(-4)	4.7(-5)	
N170	0.092	1.5(-4)	4.4(-4)	5.7(-5)	
N178	0.084	7.1(-5)	3.4(-4)	4.3(-5)	
N181 (Ty I)	0.107	6.3(-4)	4.1(-4)	1.6(-4)	
N182	0.088	2.6(-5)	2.4(-4)	3.1(-5)	
N184	0.096	7.4(-5)	3.8(-4)	5.9(-5)	6.2(-7)
N186A	0.087	5.8(-5)	4.5(-4)	9.2(-5)	1.0(-6)
N188	0.079	8.0(-5)	3.8(-4)	4.2(-5)	8.4(-7)
N192	0.098	4.2(-5)	3.8(-4)	4.9(-5)	5.8(-7)
N199 (LE)	0.042:	2.8(-5):	9.9(-5):	< 1.2(-5):	
N201 (Ty I)	0.088	8.7(-5)	1.6(-4)	1.8(-5)	
N203	0.094	1.8(-5)	4.4(-4)	5.7(-5)	
N207 (Ty I)	0.101	1.9(-4)	4.2(-4)	6.4(-5)	
N208	0.091	8.5(-5)	4.0(-4)	6.4(-5)	
N209	0.095	1.1(-4)	3.8(-4)	5.1(-5)	
N211	0.079	> 1.9(-5)	1.9(-4)	2.1(-5)::	
N212	0.098::	7.6(-6)	1.4(-4)	1.3(-5)::	
N221 (Ty I)	0.092	4.2(-4)	4.1(-4)	3.3(-5)	
LM1-9	0.088	3.0(-5)	2.1(-4)	2.4(-5)	3.6(-7)
LM1-27	0.090	9.4(-5)	3.6(-4)	6.0(-5)	1.5(-6)
LM1-61	0.082	7.8(-5)	4.1(-4)	4.5(-5)	
LM1-62	0.094	1.1(-4)	3.1(-4)	4.9(-5)	
S1 (LE)	0.090:	8.8(-6):	1.7(-4):	< 5.2(-5):	
WS12	0.079	6.1(-5)	3.5(-4)	5.4(-5)	8.8(-7)
WS16	0.115	9.4(-5)	4.4(-4)	7.8(-5)	1.6(-6)

Table 12(c). Elemental abundances for SMC PN, by number relative to hydrogen.

OBJECT	He	N	O	Ne	Ar
N1 (LE)	0.060:	1.0(-5):	8.6(-5):	< 6.7(-6):	5.2(-7):
N2	0.083		1.8(-4)	2.0(-5)	3.2(-7)
N4	0.101	2.9(-5)	2.1(-4)	1.7(-5)a	
N5	0.093	4.5(-5)	2.3(-4)	2.9(-5)	3.6(-7)
N6	0.080	3.9(-5)	1.2(-4)	1.5(-5)	4.5(-7)
N7	0.083		1.2(-4)	9.6(-6)	1.9(-7)
N18	0.070		2.0(-4)	1.9(-5)	6.6(-7)
N29 (LE)	0.067:		1.9(-4):	< 7.1(-5):	1.1(-6):
N38	0.073		1.5(-4)	2.4(-5)	3.0(-7)
N40	0.080		3.0(-4)	5.5(-5)	4.1(-7)
N42 (LE)	0.067:	4.2(-6):	1.3(-4):	< 6.2(-5):	
N43	0.074		9.9(-5)	1.5(-5)	3.0(-7)
N44	0.071		1.8(-4)	3.3(-5)	3.5(-7)
N47 (LE)	0.075:	5.6(-6):	1.9(-4):	3.5(-5):	8.4(-7):
N70	0.076	8.3(-6)	1.8(-4)	2.2(-5)a	
N87	0.091	1.1(-5)	1.1(-4)	1.0(-5)a	
L66*	0.105	1.0(-4)	6.3(-4)	6.6(-5)a	
L239	0.105	3.1(-5)	2.9(-4)	3.7(-5)	
L302 (VLE)		2.1(-5):	1.2(-4):		
L305 (Ty I)*	0.101	2.3(-4)	6.6(-5)	1.4(-5)a	
L536 (Ty I)	0.141	9.2(-5)	2.2(-5)	8.2(-6)a	

Table 13. Elemental abundances of Type I PN in the LMC and SMC, in the form log $(\overline{X/H})+12$.

	He/H	N/H	O/H	Ne/H	log (N/O)
Galactic Type I †	> 11.10				> -0.3
LMC PN					
N97	11.06	8.58	8.28	7.54	0.30
N102	11.07	8.53	8.26	7.46	0.27
N122	11.11	8.74	8.30	7.63	0.44
N181	11.03	8.80	8.61	8.20	0.19
N28	10.96	8.30	8.60	7.68	-0.30
N66	10.97	8.36	8.50	7.76	-0.14
N77F	11.00	8.64	8.64	7.70	0.00
N201	10.95	7.94	8.20	7.26	-0.26
N207	11.01	8.28	8.62	7.81	-0.34
N221	10.96	8.62	8.61	7.52	0.01
SMC PN					
L305	11.00	8.36	7.82	7.15	0.54
L536	11.15	7.96	7.34	6.91	0.62

Notes to Table 13.

† Peimbert and Torres-Peimbert, 1983.

Table 14. Mean abundances for LMC and SMC PN presented in the form log $(\overline{X/H})+12$. The mean values for all PN samples exclude Type I, VLE and LE nebulae. The standard deviation and size for each sample is given after each mean value. All He abundances have been corrected for collisional excitation.

		He	N	O	Ne	Ar	log (N/O)
SMC PN	**Full Sample**	**10.92 ±0.06 (13)**	**7.44 ±0.28 (6)**	**8.26 ±0.15 (13)**	**7.36 ±0.22 (13)**	**5.6 ±0.2 (9)**	**-0.82 ±0.25**
	He^{++} PN	10.96 ±0.04 (5)	7.54 ±0.13 (3)	8.38 ±0.10 (5)	7.51 ±0.25 (5)	5.6 ±0.1 (3)	-0.84 ±0.14
	Non He^{++} PN	10.89 ±0.04 (8)	7.30 ±0.33 (3)	8.15 ±0.15 (8)	7.26 ±0.25 (8)	5.6 ±0.2 (6)	-0.85 ±0.37
	Aller *et al.* (1981)	10.99 ±0.02 (7)	7.41 ±0.17 (7)	8.11 ±0.17 (7)	7.40 ±0.35 (7)	>5.7	-0.70 ±0.19
LMC PN	**Full Sample**	**10.94 ±0.04 (32)**	**7.81 ±0.30 (28)**	**8.49 ±0.15 (32)**	**7.64 ±0.19 (30)**	**5.9 ±0.2 (12)**	**-0.68 ±0.22**
	He^{++} PN	10.95 ±0.04 (19)	7.91 ±0.20 (18)	8.55 ±0.10 (19)	7.70 ±0.15 (19)	5.9 ±0.2 (10)	-0.64 ±0.15
	Non He^{++} PN	10.92 ±0.04 (13)	7.56 ±0.20 (10)	8.40 ±0.15 (13)	7.52 ±0.15 (11)	5.8 ±0.2 (2)	-0.84 ±0.26
	Aller (1983)	11.00 ±0.05 (6)	7.38 ±0.39 (6)	8.31 ±0.15 (6)	7.60 ±0.04 (6)	6.1 ±0.1 (6)	-0.93 ±0.42
GAL PN	Combined Sample (TPP & AC)	11.00 ±0.04 (49)	7.96 ±0.32 (43)	8.68 ±0.14 (51)	7.98 ±0.20 (45)	6.31 ±0.21 (24)	-0.76 ±0.26
	TPP †	11.00 ±0.04 (24)	8.07 ±0.32 (20)	8.80 ±0.19 (24)	8.11 ±0.27 (18)	—	-0.75 ±0.20
	AC †	10.99 ±0.05 (25)	7.85 ±0.31 (23)	8.61 ±0.17 (27)	7.95 ±0.17 (27)	6.31 ±0.21 (24)	-0.76 ±0.26
SMC H II	Table 10 (He), Pagel *et al.*(1978)	10.91 ±0.02 (3)	6.42 ±0.13 (18)	7.98 ±0.09 (23)	7.18 ±0.17 (22)	5.88 ±0.17 (10)	-1.57 ±0.10
LMC H II	Table 10 (He), Pagel *et al.*(1978)	10.91 ±0.02 (4)	6.92 ±0.15 (17)	8.39 ±0.12 (19)	7.60 ±0.15 (18)	6.33 ±0.11 (12)	-1.51 ±0.10
GAL H II	PTP77 (He) †, Dufour (1984)	11.00 ±0.02 (12)	7.57 ±0.33 (24)	8.70 ±0.25 (24)	7.90 ±0.17 (14)	6.42 ±0.23 (23)	-1.13 ±0.40
	Differences between PN and H II logarithmic abundances, mean values followed by the standard error $(\sigma/n^{1/2})$.						
SMC PN - SMC H II		0.01 ±0.02	1.02 ±0.12	0.28 ±0.05	0.18 ±0.07		
LMC PN - LMC H II		0.03 ±0.02	0.89 ±0.07	0.10 ±0.04	0.04 ±0.06		
GAL PN - GAL H II		0.00 ±0.01	0.39 ±0.07	-0.02 ±0.05	0.08 ±0.05		

† Abbreviations TPP — Torres-Peimbert and Peimbert (1977); AC — Aller and Czyzak (1983a); PTP77 — Peimbert and Torres-Peimbert (1977).

dances (specifically He/H≥0.125 and N/O≥0.5, by number). Such PN are very often bipolar in structure, with large internal motions (an example is NGC 6302) and have been interpreted as originating from the high mass end of the main sequence stellar mass range that eventually evolves through the PN phase, i.e. stars with initial masses in the range 3–5 $M_{\odot}$ (Renzini & Voli 1981; PTP83).

We have classified a number of the PN in our sample as Type I, using only the PTP83 criterion that N/O exceed 0.5 by number. Our reasons for not using the PTP83 He/H abundance criterion are two-fold. First, allowance for the effects of collisional excitation on the He I line fluxes from Galactic Type I nebulae reduces the original estimates for their He/H ratios. More importantly, however, the starting Magellanic Cloud He/H ratios are much lower than those found in the Milky Way, so that a significantly larger enhancement in the abundance of helium would be necessary before a Magellanic Cloud PN could satisfy the He/H abundance criterion for Galactic Type I PN.

A further justification for using only an N/O abundance criterion to define Type I PN is that the mean N/O ratios found for the remaining PN in the SMC, LMC and Milky Way are very similar to each other (by number, 0.15, 0.21 and 0.17, respectively; Table 14), so that the requirement that N/O exceed 0.5 represents a similar degree of nitrogen enhancement in the Type I nebulae of each galaxy.

Table 13 lists the abundances found for the 10 LMC and two SMC PN in our sample which satisfy the above Type I criterion. The two SMC Type I nebulae and the first four LMC Type I objects listed in Table 13 have N/O ratios which exceed the minimum criterion by more than a factor of 3, and so can be termed 'extreme Type I'. The Type I nature of LMC N97 was pointed out by Barlow *et al.* (1983) and by Aller (1983). Aller also remarked on the Type I characteristics of LMC N102. Webster (1976a) and Aller & Czyzak (1983b) have found that the spectrum of LMC N201 contains many lines due to [Fe VI] and [Fe VII].

One other bright Type I nebula is known to exist in the SMC, namely SMC N67 (Osmer 1976; Aller *et al.* 1987). Including SMC N67, three out of 22 SMC PN (14 per cent) are Type I, while 10 out of 50 LMC PN (20 per cent) can be classified as such. Although it has long been known that the LMC contains a higher fraction of high-excitation PN than does the SMC (Feast 1968; Webster 1975), it is not clear that the difference in the fractions of Type I nebulae is statistically significant.

The neon abundances found for the Type I PN (Table 13) appear normal relative to the other PN in their galaxies (Table 14). The mean oxygen abundance found for the 10 LMC Type I nebulae (8.46±0.18) likewise appears normal relative to that of other LMC PN (8.49±0.15; Table 14). However, the oxygen abundances derived for SMC L305 and SMC L536 (Table 13) appear to be significantly lower than the oxygen abundance found for other PN or H II regions in the SMC (Table 14). The other bright Type I nebula in the SMC (N67) has also been found to have a significantly reduced oxygen abundance (7.15, where $H=12.0$; Aller *et al.* 1987). This may indicate that oxygen has been destroyed by the ON cycle, so the Type I nebulae in the SMC deserve further study.

9 Mean abundances for N, O, Ne and Ar

In Table 14 we present the mean abundances of helium, nitrogen, oxygen, neon and argon for the LMC and SMC PN in this survey. These were calculated by excluding the Type I objects, the low- and very-low-excitation objects (Ty I, LE and VLE in Tables 9, 11 and 12), and all abundances shown as uncertain (::) or as an upper or lower limit. The abundances are presented in the form $\log X/H+12$, followed by the standard deviation, and (in parentheses) the number of objects in each sample.

The second column of Table 14 gives the reference for each dataset and, for data presented in this paper, whether the sample was for PN with an observed He II 4686 Å line ('He^{2+} PN'), for PN without an observed He II 4686 Å line ('Non-He^{2+} PN'), or for all PN ('Full sample'). The final three rows of Table 14 give the differences between the abundances in PN and H II regions in each of the LMC, SMC and our own Galaxy, as derived from the adopted mean abundances for each galaxy.

Our helium abundances include an allowance for the contribution made by collisional excitations from He I 2^3S (see Section 6). This also affects the derived abundances of N, O and Ne, through the ICFs (see Section 7). The percentage change in the abundances of N, O and Ne, for calculations excluding the collisional excitation of He I compared with those including this mechanism, is of the order of 6 per cent, a negligible variation compared to the scatter about the means. The allowance for collisional excitation of He I decreases the mean helium abundance by approximately 20 per cent for the 'full sample', by 14 per cent for the 'He^{2+} PN' sample, and by 26 per cent for the 'Non-He^{2+} PN' sample.

Inspection of the mean abundances in Table 14 shows that, for both the SMC and LMC, the elemental abundances found for He^{2+} PN are always larger than those found for non-He^{2+} PN. In most cases the differences are within the total error limits but the differences for helium in the SMC and nitrogen in the LMC appear significant, as does the fact that there are no examples of an element being more abundant in non-He^{2+} PN. Since ICFs are often larger for He^{2+} PN, one might suspect their reliability, particularly for nitrogen, whose abundances are based on fairly large ICFs applied to the abundance of N^+. However, whenever the ICF method has been directly checked by ultraviolet observations (e.g. Barker 1983), the method has been found to be reliable. Fig. 3 shows a plot of the nitrogen ICFs for all of the LMC PN, with the He^{2+} PN indicated by filled symbols and non-He^{2+} PN indicated by open symbols. Although there is a clear separation in their nitrogen abundances, this does not appear to be attributable to their ICFs.

If the elemental enhancements in the He^{2+} PN are indeed real, then it may be possible to interpret them as due to their progenitor stars being slightly more massive and younger than those of the non-He^{2+} group. If more massive, such stars could have higher initial abundances and

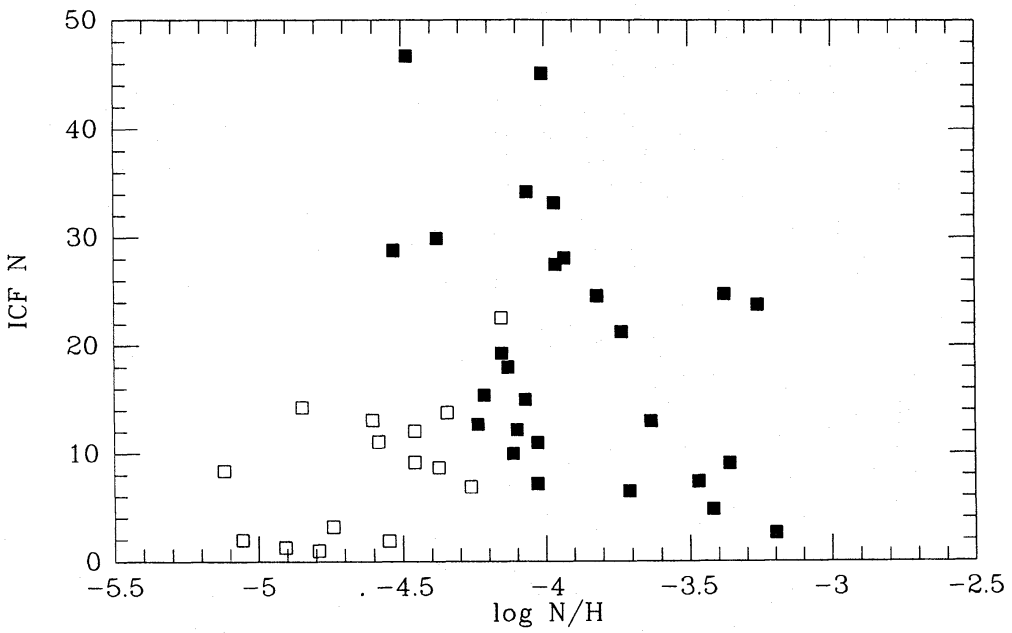

Figure 3. A plot of log N/H (on a scale where log H=12.0) versus the nitrogen ionization correction factor (ICF N), for LMC PN. The open squares are nebulae without He II 4686 Å present in their spectra, whilst the filled squares are nebulae with He II 4686 Å. The Type I objects all have log N/H≥−3.7.

might self-enrich themselves in He and N to a greater extent. As central stars, they would also evolve more quickly, making it more probable to find them at the higher effective temperatures characteristic of the He^{2+} PN.

In order to compare the present abundances with those of previous studies it was necessary to correct the earlier results for the effects of collisional excitation of He I. For this purpose, the samples of Aller (1983), Aller *et al.* (1981), Torres-Peimbert & Peimbert (1977) and Aller & Czyzak (1983a) were used (excluding Type I and low-excitation PN). The reduction in the ionic abundance of He^+ due to collisional excitation was estimated using the equations of Clegg (1987), employing the same T_e, n_e, and general methods as the original authors. The resulting corrected mean abundances are also presented in Table 14. No correction was applied to the adopted heavy element abundances in Table 14 of H II regions in the LMC, SMC and our own Galaxy (Pagel *et al.* 1978) since the electron temperatures and densities in these regions lead to little collisional excitation of He I (see Table 10) and therefore negligible changes to the ICFs.

A comparison of the mean abundances found here (i.e. the 'full sample' abundances of Table 14) with those of Aller (1983) for LMC PN, and those of Aller *et al.* (1981) for SMC PN, shows that there is good general agreement, within the errors, between the results. Due to our much larger sample, the abundances calculated in this paper are adopted as the means. It should be noted, though, that the mean nitrogen abundance found for the SMC PN could be an upper limit due to selection effects, since the eight SMC PN for which no [N II] was detectable in low resolution spectra could be objects with lower nitrogen abundances.

If one compares the abundances found here for Magellanic Cloud PN with those found previously for Galactic PN (Table 14), one finds that the abundances of neon and argon, the elements least affected by nucleosynthesis during the evolution of the PN progenitor star, are lower by 0.6 and 0.35 dex, for the SMC and LMC respectively. Oxygen is found to be lower by 0.4 and 0.2 dex in SMC and LMC PN relative to those in our own Galaxy. Within the errors, the oxygen and neon abundances in Magellanic Cloud PN are the same as those previously found for H II regions in the SMC and LMC.

The final column of Table 14 gives the relative abundance of nitrogen to oxygen (log N/O) for PN and H II regions in the LMC, SMC, and our own galaxy. It is noticeable that the mean values of log N/O for SMC, LMC and Galactic PN are all similar (−0.82, −0.68 and −0.76, respectively), whilst the SMC and LMC H II region log N/O ratios are quite different from the Galactic ratio (−1.56, −1.46 and −1.13, respectively).

Comparing the elemental abundances found for LMC PN and the LMC H II regions (Table 14), it can be seen that there has been significant enrichment of nitrogen, by 0.89 dex, whilst the abundances of helium, oxygen, neon and argon are unchanged within the error limits. A similar comparison for the SMC shows an increase by 1.02 dex of the nitrogen abundance in the PN, while again the helium, oxygen, neon, and argon abundances remain the same within the error limits. The extent of the nitrogen enhancements in the LMC and SMC PN is significant, more so when compared with our own Galaxy, where the PN show a nitrogen enhancement (compared to H II regions) of only 0.38 dex.

The clear enhancement of nitrogen in Magellanic Cloud PN appears to be consistent with the exposure at the surfaces of the PN progenitor stars of the main product of the CN cycle, namely secondary nitrogen produced by conversion of the initial carbon. Such an effect (the 'first dredge-up') is predicted to occur early in the post-main sequence life of all low- and intermediate-mass stars (Iben & Renzini 1983). Becker & Iben (1980) have predicted that, following the first dredge-up, about one-third of the initial carbon should have been converted to nitrogen for low-mass stars of solar composition, while for low-mass stars of Population II composition, the fraction of carbon converted to nitrogen should be about unity. Our results appear to be consistent with this. The abundances listed in Table 15 are the same as those listed in Table 14, supplemented by the

Table 15. The CN cycle in Magellanic Cloud and Galactic PN.

	Mean logarithmic abundances, H = 12.0				
	C	N	C+N	O	Ne
SMC PN		**7.44±0.28**		8.26 ± 0.15	7.36 ± 0.22
SMC H II	7.16 ± 0.04	6.42 ± 0.13	**7.23±0.14**	7.98 ± 0.09	7.18 ± 0.17
LMC PN		**7.81±0.30**		8.49 ± 0.15	7.64 ± 0.19
LMC H II	7.90 ± 0.15	6.92 ± 0.15	**7.94±0.20**	8.39 ± 0.12	7.60 ± 0.15
GAL PN		**7.96±0.32**		8.68 ± 0.14	7.98 ± 0.20
GAL H II	8.46	7.57 ± 0.33	**8.51±0.35**	8.70 ± 0.25	7.90 ± 0.17

H II region carbon abundances of Dufour *et al.* (1982). The fourth column of Table 15 lists the sum of the abundances of C and N for H II regions in the SMC, LMC and Milky Way, respectively. For the SMC, whose heavy element abundances are comparable to those of Population II stars, we see that all of the initial carbon must have been converted to nitrogen in order to match the PN nitrogen abundances. For our own Galaxy, the figures in Table 15 imply that about 20 per cent of the initial carbon has been converted to nitrogen in the PN, while in the LMC, whose abundances are intermediate between those of the Milky Way and SMC, the fraction of initial carbon converted to nitrogen is 70 per cent. Although the CN cycle appears to have operated to near-completion in the SMC and LMC PN, there is no evidence for any depletion of oxygen caused by the ON cycle.

It should be noted that although the nebular carbon abundances in Magellanic Cloud PN can show great enhancements (Maran *et al.* 1982; Aller *et al.* 1987), these enhancements can be interpreted as due to the effects of the 'third dredge-up' (Iben & Renzini 1983), whereby the products of the triple-α reaction are brought to the surface much later in the evolution of the progenitor stars.

Acknowledgments

DJM thanks the Science and Engineering Research Council and the Perrin Fund at UCL for support during the period of this research. We also wish to acknowledge very helpful correspondence with Dr E. J. Wampler.

References

Adams, S. 1983. *PhD thesis,* University College London.
Aller, L. H., 1983. *Astrophys. J.*, **273,** 590.
Aller, L. H. & Czyzak, S. J., 1983a. *Astrophys. J. Suppl.*, **51,** 211.
Aller, L. H. & Czyzak, S. J., 1983b. *Proc. natn. Acad. Sci. USA.*, **80,** 1764.
Aller. L. H., Keyes, C. D., Ross, J. E. & O'Mara, B. J., 1981. *Mon. Not. R. astr. Soc.*, **194,** 613.
Aller, L. H., Keyes, C.D., Maran, S. P., Gull, T. R., Michalitsianos, A. G. & Stecher, T. P., 1987. *Astrophys. J.*, **320,** 159.
Baluja, K. L., Burke, P. G. & Kingston, A. E., 1980. *J. Phys. B,* **13,** 829.
Barker, T., 1980. *Astrophys. J.*, **240,** 99.
Barker, T., 1983. *Astrophys. J.*, **267,** 630.
Barlow, M. J., 1987. *Mon. Not. R. astr. Soc.*, **227,** 161.

Barlow, M. J., Adams, S., Seaton, M. J., Willis, A. J. & Walker, A. R., 1983. *IAU Symp. No. 103,* p. 538, ed. Flower, D. R., Reidel, Dordrecht, Holland.
Becker, S. A. & Iben, I., Jr, 1980. *Astrophys. J.,* **237,** 129.
Berrington, K. B., Burke, P. G., Freitas, L. C. G. & Kingston, A. E., 1985. *J. Phys. B,* **18,** 4135.
Berrington, K. B. & Kingston, A. E., 1987. *J. Phys. B,* **20,** 6631.
Brocklehurst, M., 1971. *Mon. Not. R. astr. Soc.,* **153,** 471.
Brocklehurst, M., 1972. *Mon. Not. R. astr. Soc.,* **157,** 211.
Butler, K. & Mendoza, C., 1984. *Mon. Not. R. astr. Soc.,* **208,** 17P.
Clegg, R. E. S., 1987. *Mon. Not. R. astr. Soc.,* **229,** 31P.
Clegg, R. E. S., Seaton, M. J., Peimbert, M. & Torres-Peimbert, S., 1983. *Mon. Not. R. astr. Soc.,* **205,** 417.
Dufour, R. J., 1984. *IAU Symp. No. 108,* p. 353, eds van der Bergh, S. & de Boer, K. S., Reidel, Dordrecht, Holland.
Dufour, R. J. & Killen, R. M., 1977. *Astrophys. J.,* **211,** 68.
Dufour, R. J., Shields, G. A. & Talbot, R. J., 1982. *Astrophys. J.,* **252,** 461.
Feast, M. W., 1968. *Mon. Not. R. astr. Soc.,* **140,** 345.
Ferland, G. J., 1986. *Astrophys. J.,* **310,** L67.
Fleming, T. A., Liebert, J. & Green, R. F., 1986. *Astrophys. J.,* **308,** 176.
Henize, K. G., 1956. *Astrophys. J. Suppl.,* **2,** 315.
Henize, K. G. & Westerlund, B. E., 1963. *Astrophys. J.,* **137,** 747.
Howarth, I. D., 1983. *Mon. Not. R. astr. Soc.,* **203,** 301.
Howarth, I. D. & Murray, J., 1987. *Starlink User Note No. 50.*
Hummer, D. G. & Storey, P. J., 1987. *Mon. Not. R. astr. Soc.,* **224,** 801.
Iben, I., Jr & Renzini, A., 1983. *Ann. Rev. Astr. Astrophys.,* **21,** 271.
Jacoby, G. H., 1980. *Astrophys. J. Suppl.,* **42,** 1.
Kaler, J. B., 1978. *Astrophys. J.,* **226,** 947.
Krueger, T. K. & Czyzak, S. J., 1970. *Proc. R. Soc. Lond. A,* **318,** 531.
Liebert, J., 1986. *Proc. IAU Colloq. No. 87,* p. 367, eds Hunger, K. & Schoenberner, D., Reidel, Dordrecht, Holland.
Lindsay, E. M., 1961. *Astrophys. J.,* **66,** 169.
Lindsay, E. M. & Mullan, D. J., 1963. *Irish astr. J.,* **6,** 51.
Maran, S. P., Aller, L. H., Gull, T. R. & Stecher, T. P., 1982. *Astrophys. J.,* **253,** L43.
Mendez, R. H., Miguel, C. H., Heber, U. & Kudritzki, R. P., 1986. *Proc. IAU Colloq. No. 87,* p. 323, eds Hunger, K. and Schoenberner, D., Reidel, Dordrecht, Holland.
Mendoza, C., 1983. *IAU Symp. No. 103,* p. 233, ed. Flower, D., Reidel, Dordrecht, Holland.
Mendoza, C. & Zeippen, C. J., 1982. *Mon. Not. R. astr. Soc.,* **198,** 127.
Mendoza, C. & Zeippen, C. J., 1983. *Mon. Not. R. astr. Soc.,* **202,** 981.
Monk, D. J., 1987. *PhD thesis,* University College London.
Morgan, D. H., 1984. *Mon. Not. R. astr. Soc.,* **208,** 633.
Nussbaumer, H. & Rusca, C., 1979. *Astr. Astrophys.,* **72,** 129.
Nussbaumer, H. & Storey, P. J., 1981. *Astr. Astrophys.,* **99,** 177.
Oke, J. B., 1974. *Astrophys. J. Suppl.,* **27,** 21.
Osmer, P. S., 1976. *Astrophys. J.,* **203,** 352.
Pagel, B. E. J., Edmunds, M. G., Fosbury, R. A. E. & Webster, B. L., 1978. *Mon. Not. R. astr. Soc.,* **184,** 569.
Peimbert, M. & Torres-Peimbert, S., 1971. *Astrophys. J.,* **168,** 413.
Peimbert, M. & Torres-Peimbert, S., 1977. *Mon. Not. R. astr. Soc.,* **179,** 217.
Peimbert, M. & Torres-Peimbert, S., 1983. *IAU Symp. No. 103,* p. 233, ed. Flower, D., Reidel, Dordrecht, Holland.
Peimbert, M. & Torres-Peimbert, S., 1987. *Rev. Mex. Astr. Astrof.,* **14,** 540.
Pradhan, A. K., 1976. *Mon. Not. R. astr. Soc.,* **177,** 31.
Renzini, A. & Voli, M., 1981. *Astr. Astrophys.,* **94,** 175.
Robinson, L. B. & Wampler, E. J., 1972. *Publ. astr. Soc. Pacif.,* **84,** 161.
Rosa, M., 1985. *ESO Messenger,* **39,** 15.
Sanduleak, N. & Philip, A. G. D., 1977. *Publs astr. Soc. Pacif.,* **89,** 792.
Sanduleak, N., MacConnell, D. J. & Philip, A. G. D., 1978. *Publ. astr. Soc. Pacif.,* **90,** 621.
Sanduleak, N. & Stephenson, C. B., 1972. *Astrophys. J.,* **178,** 183.
Seaton, M. J., 1975. *Mon. Not. R. astr. Soc.,* **170,** 475.
Smith, L. F. & Aller, L. H., 1971, *Astrophys. J.,* **164,** 275.
Smith, M. J. & Weedman, D. W., 1972. *Astrophys. J.,* **177,** 595.
Stecher, T. P., Maran, S. P., Gull, T. E., Aller, L. H. & Savedoff, M. P., 1982. *Astrophys. J.,* **262,** L41.
Straede, J., 1980. *A.A.O. Preprint No. 135.*

Torres, A. N., Conti, P. S. & Massey, P., 1986. *Astrophys. J.*, **300,** 379.
Torres-Peimbert, S. & Peimbert, M. 1977. *Rev. Mex. Astr. Astrof.*, **2,** 181.
Webster, B. L., 1969a. *Mon. Not. R. astr. Soc.*, **143,** 79.
Webster, B. L., 1969b. *Mon. Not. R. astr. Soc.*, **143,** 97.
Webster, B. L., 1975. *Mon. Not. R. astr. Soc.*, **173,** 437.
Webster, B. L., 1976a. *Mon. Not. R. astr. Soc.*, **174,** 513.
Webster, B. L., 1976b. *Publ. astr. Soc. Pacif.*, **88,** 669.
Webster, B. L., 1978. *IAU Symp. No. 76,* p. 215, ed. Terzian, Y., Reidel, Dordrecht, Holland.
Westerlund, B. E. & Smith, L. F., 1964. *Mon. Not. R. astr. Soc.*, **127,** 449.
Wood, P. R. & Faulkner, D. J., 1986. *Astrophys. J.*, **307,** 659.
Zeippen, C., 1982. *Mon. Not. R. astr. Soc.*, **198,** 111.
Zeippen, C., Butler, K. & Le Bourlot, J., 1987. *Astr. Astrophys.*, **188,** 251.